Journal of the Mechanics and Physics of Solids 59 (2011) 561–582

Contents lists available at ScienceDirect

Journal of the Mechanics and Physics of Solids

journal homepage: www.elsevier.com/locate/jmps

Inhomogeneous deformation of elastomer gels in equilibrium under saturated and unsaturated conditions

S. Baek *, T.J. Pence

Department of Mechanical Engineering, 2500 Engineering Building, Michigan State University, East Lansing, MI 48824-1226, United States

ARTICLE INFO

Article history:
Received 10 September 2010
Accepted 19 December 2010
Available online 23 December 2010

Keywords:
Swelling
Hydrogel
Interface conditions
Loss-of-saturation
Chemical potential in mechanochemistry

ABSTRACT

A variational method is employed to obtain governing equations and boundary conditions describing finite strain equilibrium configurations of elastomeric gels. Three situations are considered: a liquid saturated gel, an unsaturated gel, and a gel in equilibrium with a vapor of its own liquid. Surface tractions can lead to equilibrium transitions between these cases. The liquid saturated gel is regarded as immersed in a liquid bath. If this bath becomes depleted, then the gel is unsaturated. The degree of unsaturation – a measure of the amount of liquid that would restore a state of saturation – affects the subsequent mechanical behavior. If the unsaturated system is further allowed to condense or evaporate its liquid component at the gel surface, then a new state of equilibrium is achieved. The transition between the unsaturated case and the case of being in equilibrium with the vapor phase corresponds to the chemical potential variable of the gel changing its value from one that is determined by a volume constraint to the value of the chemical potential in the vapor phase. A finite element method is created on the basis of the variational method and demonstrated in the context of eversion, a deformation that imposes very large finite strains. Liquid migration within the gel is not modeled as our focus is on equilibrium states that occur after all such non-equilibrium processes come to rest.

1. Introduction

A gel is a mixture of crosslinked polymer chains and an interpenetrating fluid. Because of their solid-like properties and the ability to contain a large amount of a liquid, gels have numerous applications including areas such as tissue engineering (Lee and Mooney, 2001; Nguyen and West, 2002) and drug delivery (Qiu and Park, 2001; Gupta et al., 2002). When an external force is applied to such a gel, the fluid diffuses in or out from the swollen solid and the volume of the body changes. Eventually, when the diffusion process is completed, the body maintains equilibrium with the external force by virtue of the elastic stresses arising from the deformation. Many of these stresses are entropic in nature as they arise both from the mixing of the solid and liquid constituents, and from the configurational entropy changes of the crosslinked polymer chains. From these observations, Treloar (1975) pointed out that the equilibrium mechanical properties of the gel correspond to those of a compressible material made up of a single constituent, even when the individual constituents – the polymer and the fluid – are each incompressible.

To describe the mechanical behavior of an elastomeric gel in a quantitative fashion, theoretical models have been developed using variational methods based on the thermodynamics of mixtures (see for example: Huggins, 1942; Flory and

* Corresponding author. Tel.: +1 517 432 3161.
E-mail address: sbaek@egr.msu.edu (S. Baek).

0022-5096/$ - see front matter © 2010 Elsevier Ltd. All rights reserved.
doi:10.1016/j.jmps.2010.12.013

Rehner, 1943; Treloar, 1950; Bowen, 1980, 1982; Gandhi et al., 1987, 1989; Rajagopal and Tao, 1996; Baek and Srinivasa, 2004a; Hong et al., 2008; Duda et al., 2010). In particular, such a gel is in equilibrium only if its free energy is a minimum with respect to both changes in the mass fraction of the individual constituents and to the deformation of the solid constituent. For large deformation the latter type of variation naturally lends itself to a hyperelastic treatment, whereas the former type of variation involves liquid flux across the gel boundary and liquid redistribution within the gel.

If the amount of liquid is limited it can then be the case that certain loadings cause all of the liquid component to enter into the gel. If this is the case then the gel is no longer saturated and such a gel is referred to here as unsaturated. Specifically, if an additional small amount of liquid is brought into contact with such an unsaturated gel then that liquid, upon being absorbed by the gel, allows the system to establish a lower free energy for the same state of mechanical loading. Under such a process the gel remains unsaturated under repeated introduction of a small amount of liquid so long as the liquid continues to be absorbed. Once equilibrium is attainable with no additional liquid absorption then the gel is once again saturated. Such considerations apply to both homogeneous and inhomogeneous deformation. For homogeneous deformation the liquid is uniformly distributed within the gel, so that any liquid introduced to the unsaturated gel also becomes uniformly distributed after liquid diffusion is complete and equilibrium subsequently attained. In contrast, for inhomogeneous deformation the liquid is generally not uniformly distributed.

This concept of saturation is discussed in the book by Rajagopal and Tao (1996), and the notion of saturation boundary conditions is developed by Rajagopal, Wineman and collaborators in a variety of papers in the 1980s and 90s.[1] They do not, however, systematically consider the notion of a transition between equilibrium states, one of which is saturated and the other of which is not saturated. Nor do they examine the effect of what one may regard as the amount of undersaturation due to differing overall quantities of liquid in an unsaturated gel. Such issues have recently been studied by Deng and Pence (2010a,b), where it is shown how, generally, a loss-of-saturation transition renders the system mechanically stiffer than that of a corresponding saturated system. Such stiffness increases with the amount of undersaturation.

One of the difficulties in developing a theoretical framework for modeling gels under such circumstances is related to the standard and reasonable approximation that all of the volume change in the gel is due exclusively to fluid mass transfer. In the usual variational treatment this constraint results in a Lagrange multiplier which then appears in the expressions for the stress and the chemical potential. As discussed by Baek and Srinivasa (2004a), the use of the Lagrange multiplier technique can obscure the physical interpretation of the resulting balance expressions and hinders the identification of appropriate boundary conditions. To clarify these issues, the treatment in Baek and Srinivasa (2004a) reformulates the variational problem so that it is initially without such a constraint. Then a limiting process is employed such that departure from the constraint is increasingly penalized. The resulting variational formulation – which applies to the notion of a saturated gel as discussed above – takes the system to be the gel with its surrounding fluid bath. By including the fluid bath, the limiting procedure provides a means for obtaining the equilibrium boundary conditions at the interface between the gel and the bath.

In this work, we employ this variational approach to treat both saturated and unsaturated gels in equilibrium and subject to loading at the gel surface. Body forces are neglected and so in particular the effect of gravity is not addressed. We also restrict attention to isothermal processes so that temperature either need not enter the treatment or, more generally, is regarded as a parameter. The constitutive theory requires knowledge of the free energy of the gel ψ_g and of the surrounding fluid ψ_f. Since we confine attention to equilibrium states, there is no need to specify constitutive entities associated with the dynamical processes that take place prior to attaining equilibrium (e.g., diffusion) and for this reason it is not necessary to specify a constitutive form for the rate of dissipation as is done in Baek and Srinivasa (2004a). Here a variational formulation is obtained for three separate and related situations. The first is that of a saturated gel, meaning a gel that is in equilibrium with applied surface tractions while also within a liquid bath (the saturated gel referred to above). The second is that of an unsaturated gel in the sense already described, meaning that there is no longer a source for additional liquid to enter into the gel even though maintaining saturation under surface tractions would require such a liquid source. The third is that of gel subject to surface tractions that is in equilibrium with a vapor of the same substance as that which constitutes the liquid component of the gel. Both the liquid bath in the first situation, and the surrounding vapor in the third situation, will generally have an associated pressure. Different boundary conditions at the gel surface are obtained from the variational procedure for these different situations. In particular, the procedure clarifies the role of the gel chemical potential in each of these differing situations. In addition, we show how the theoretical framework employed in Deng and Pence (2010a,b) emerges naturally from the variational procedure for the first two situations enumerated above. This is especially useful since the framework as employed in Deng and Pence (2010a,b) proceeded on the basis of hyperelasticity and specifically involved no explicit mention of the chemical potential concept. Thus, even though the framework of Deng and Pence (2010a,b) does not specifically identify a chemical potential, it remains consistent with mixture theory treatments that specifically identify such an entity. All of these considerations are developed in Sections 3 and 4.

The variational formulation is then used to construct a finite element formulation for two situations of a saturated gel and an unsaturated gel. The accuracy of the finite element procedure is demonstrated for the special case of an everted gel cylinder (turning a short tube inside-out). The special case of eversion with specialized end tractions that make the everted

[1] We also remark that the way in which the term saturation is used in the present paper may be different from other ways in which the term is used in the context of continuum mixture theories. For example, in Ambrosi et al. (2010) saturation is used to mean that the volume fraction of all constituents must sum to unity, which is different from our use of the term.

shape a perfect cylinder was reduced to the consideration of ODEs in Deng and Pence (2010a) and solved numerically. The finite element procedure presented here faithfully replicates these cylindrically symmetric solutions for both the saturated and the unsaturated case. Then the finite element procedure is demonstrated on eversion problems that do not maintain perfect cylinders upon eversion (and which are thus not treatable by the ODE method in Deng and Pence, 2010a). In particular, everted cylinders that are completely free of surface tractions will generally flare out a bit at the top and bottom. This is confirmed by the finite element procedure, and the effect of differing amounts of gel undersaturation is quantified in this regard. Finally, the finite element method (FEM) is used to simulate the full eversion sequence itself by prescribing a set of cap displacements that have the effect of turning the cylinder inside-out.

2. The liquid saturated gel: A gel in contact with a fluid bath

As stated in the Introduction, a gel is mixture of solid (polymer) and liquid constituents. Fig. 1 shows a liquid saturated gel occupying domain Ω_g. It is surrounded by a bath of the same fluid which occupies domain Ω_f. The surface of the gel is Γ_g which is therefore also the interface between the gel and the fluid bath. This surface is defined by locations of the solid polymer component, thus fluid may transfer between the gel and the bath at Γ_g. The boundary of the fluid bath consists of Γ_g and the bath's external boundary Γ_{ext}. The boundary Γ_{ext} is defined by fluid particle locations, hence fluid may not cross Γ_{ext}. The boundary Γ_{ext} is in turn subdivided into two parts: Γ_{con} giving the boundary of the container holding the bath, and Γ_f where the fluid is in contact with external pressure p_{app}. All of these domains and boundaries are in the current and hence deformed configuration. On the gel surface Γ_g there may be external mechanical tractions $\mathbf{t}$ that are applied directly to the gel. External body forces are not considered.

The variable $\mathbf{x}$ denotes spatial position in the current configuration; as such $\mathbf{x}$ is independent of the movement of the fluid and the gel constituents. Locations within the gel are determined by tracking the position of its solid (polymer) component. These locations are denoted by $\mathbf{x}_g$. The relative movement of fluid particles within the gel is considered as a mass flux. The deformation of the solid component of the gel stores and releases elastic energy and so a reference configuration is introduced for the solid component of the gel. We take this reference configuration to be a nominally dry polymer state prior to uptake of the liquid, and we let $\mathbf{X}_g$ be the position of the solid component in this reference configuration. Then the displacement and deformation gradient of the gel are, respectively, given by

$$\mathbf{u}_g = \mathbf{x}_g - \mathbf{X}_g, \quad \mathbf{F} = \frac{\partial \mathbf{x}_g}{\partial \mathbf{X}_g}. \tag{1}$$

The density of the gel in Ω_g and the density of the fluid in Ω_f are ρ_g and ρ_f, respectively. As regards the fluid, we shall eventually assume the fluid to be incompressible with constant density ρ_{f0}. However, following Baek and Srinivasa (2004a), this requirement is not imposed at the outset. As regards the gel, we shall eventually assume that the current volume of the swollen gel is the sum of the volume of its solid component and the volume of absorbed fluid. This assumption is called the "volume additivity constraint" in Rajagopal and Tao (1996), and it has recently also been called "molecular incompressibility" in Hong et al. (2008). When both liquid incompressibility and volume additivity hold it then follows that

$$\rho_g = \frac{1}{J}\rho_{s0} + \left(1 - \frac{1}{J}\right)\rho_{f0}, \tag{2}$$

where ρ_{s0} is the constant density of the dry polymer and $J = \det\mathbf{F}$. While Eq. (2) is typically used as a local constraint, Baek and Srinivasa (2004a) discuss how this constraint can obscure many of the thermodynamical features that are central to understanding the gel's mechanical behavior. Accordingly, they first develop the theory in the absence of any such constraint, and then obtain the theory in which these constraints hold by means of a limiting process. We follow that development here as well. Thus neither fluid incompressibility nor volume additivity is imposed at this point in the development.

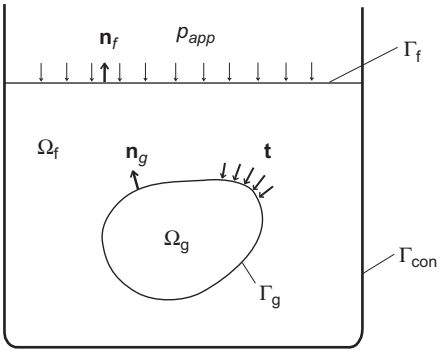

Fig. 1. The system consists of the domain Ω_g for a gel and Ω_f for a surrounding fluid in the bath. These two domains are separated by the interface Γ_g and fluid may transfer at the interface. The external boundary of the bath is denoted by $\Gamma_{ext} = \Gamma_{con} \bigcup \Gamma_f$. An external pressure p_{app} is applied to the fluid on Γ_f and an external traction $\mathbf{t}$ is applied to the gel on Γ_g.

The swollen gel and the surrounding fluid are each characterized by a Helmholtz free energy per unit volume in the current configuration. In the fluid bath this energy is dependent upon density and temperature. Since we are considering isothermal conditions, this fluid free energy is written simply as $\psi_f(\rho_f)$. The Helmholtz free energy of the gel ψ_g depends not only upon its density, but also upon the deformation of the polymeric component and so is of the form $\psi_g(\mathbf{F},\rho_g)$. In addition, the principle of frame-indifference requires that the dependence of ψ_g upon $\mathbf{F}$ is reducible to a dependence upon $\mathbf{C}=\mathbf{F}^T\mathbf{F}$, however, it is convenient to defer the use of this fact until after the equations of equilibrium are formally obtained.

2.1. The variational approach

The equations of equilibrium are now obtained by a variational argument in which the gel is subject to displacement variations $\delta\mathbf{u}_g$ and the fluid is subject to displacement variations $\delta\mathbf{u}_f$. Recall that $\mathbf{u}_g$ gives the displacement of the solid component of the gel. The fluid within the gel will exhibit variations as well, and these are described by the fluid mass displacement $\delta\mathbf{q}$ within the gel relative to the displacement of the solid component $\delta\mathbf{u}_g$. Admissible variations $\{\delta\mathbf{u}_g,\delta\mathbf{q},\delta\mathbf{u}_f\}$ have $\delta\mathbf{u}_f=\mathbf{0}$ on Γ_{con} and must also account for mass flux continuity across the gel boundary Γ_g which gives

$$\rho_f(\delta\mathbf{u}_f-\delta\mathbf{u}_g)=\delta\mathbf{q} \quad \text{on } \Gamma_g. \tag{3}$$

By virtue of mass conservation, the variations $\{\delta\mathbf{u}_g,\delta\mathbf{q}\}$ gives rise to a density variation $\delta\rho_g$ in the gel obeying

$$\delta\rho_g+\mathrm{div}(\rho_g\delta\mathbf{u}_g)+\mathrm{div}(\delta\mathbf{q})=0 \quad \text{in } \Omega_g. \tag{4}$$

In a similar fashion, the variation $\delta\mathbf{u}_f$ gives rise to a density variation $\delta\rho_f$ in the fluid bath obeying

$$\delta\rho_f+\mathrm{div}(\rho_f\delta\mathbf{u}_f)=0 \quad \text{in } \Omega_f. \tag{5}$$

For all admissible variations $\{\delta\mathbf{u}_g,\delta\mathbf{q},\delta\mathbf{u}_f\}$ it is now required that $\delta\Pi=0$ where

$$\delta\Pi=\delta\left(\int_{\Omega_g}\psi_g\,dV+\int_{\Omega_f}\psi_f\,dV\right)-\int_{\Gamma_g}\mathbf{t}\cdot\delta\mathbf{u}_g\,dA+\int_{\Gamma_f}p_{app}\mathbf{n}_f\cdot\delta\mathbf{u}_f\,dA. \tag{6}$$

Here $\mathbf{n}_f$ is the outward normal vector on Γ_f. By Leibniz's rule, the first term in the right hand side of (6) becomes

$$\delta\left(\int_{\Omega_g}\psi_g\,dV+\int_{\Omega_f}\psi_f dV\right)=\int_{\Omega_g}\delta\psi_g\,dV+\int_{\Gamma_g}(\psi_g-\psi_f)\delta\mathbf{u}_g\cdot\mathbf{n}_g\,dA+\int_{\Omega_f}\delta\psi_f\,dV+\int_{\Gamma_f}\psi_f\delta\mathbf{u}_f\cdot\mathbf{n}_f\,dA, \tag{7}$$

where $\mathbf{n}_g$ is the normal vector on Γ_g pointing from the gel into the bath. The variations $\delta\psi_g$ and $\delta\psi_f$ are formally given by

$$\delta\psi_g=\frac{\partial\psi_g}{\partial\mathbf{F}}:\delta\mathbf{F}+\frac{\partial\psi_g}{\partial\rho_g}\delta\rho_g, \quad \delta\psi_f=\frac{\partial\psi_f}{\partial\rho_f}\delta\rho_f, \tag{8}$$

where $\delta\rho_f$ and $\delta\rho_g$ follow immediately from (4) and (5). As regards the tensor $\delta\mathbf{F}$ note that the variation of $\mathbf{F}$ at a fixed gel particle location $\mathbf{x}_g$ follows from the chain rule as $\delta\mathbf{F}|_{(\text{fixed }\mathbf{x}_g)}=(\mathrm{grad}\,\delta\mathbf{u}_g)\mathbf{F}$. However it is important to realize that the variation $\delta\psi_g$ in (8) is at fixed spatial location $\mathbf{x}$ which in turn requires that $\delta\mathbf{F}$ in (8) is also a variation at fixed $\mathbf{x}$. For scalar functions f the variations at fixed $\mathbf{x}$ and fixed $\mathbf{x}_g$ are connected by the "convected derivative" like identity

$$\delta f|_{(\text{fixed }\mathbf{x}_g)}=\delta f|_{(\text{fixed }\mathbf{x})}+(\mathrm{grad}f)\cdot\delta\mathbf{u}_g, \tag{9}$$

with similar relations for vector and tensor functions. This gives $\delta\mathbf{F}|_{(\text{fixed }\mathbf{x})}=\delta\mathbf{F}|_{(\text{fixed }\mathbf{x}_g)}-(\mathrm{grad}\mathbf{F})\delta\mathbf{u}_g$ so that $\delta\mathbf{F}$ in (8) is given by

$$\delta\mathbf{F}=(\mathrm{grad}\,\delta\mathbf{u}_g)\mathbf{F}-(\mathrm{grad}\mathbf{F})\delta\mathbf{u}_g. \tag{10}$$

It therefore follows from (4), (5), (8), and (10) that

$$\delta\psi_g=\frac{\partial\psi_g}{\partial\mathbf{F}}:\{(\mathrm{grad}\,\delta\mathbf{u}_g)\mathbf{F}-(\mathrm{grad}\,\mathbf{F})\delta\mathbf{u}_g\}-\frac{\partial\psi_g}{\partial\rho_g}\{\mathrm{div}(\rho_g\delta\mathbf{u}_g)+\mathrm{div}(\delta\mathbf{q})\} \quad \text{in } \Omega_g, \tag{11}$$

$$\delta\psi_f=-\frac{\partial\psi_f}{\partial\rho_f}\{\mathrm{div}(\rho_f\delta\mathbf{u}_f)\} \quad \text{in } \Omega_f. \tag{12}$$

Substituting from (7), (11), (12) into (6) one finds, after application of the divergence theorem and use of (3), that $\delta\Pi$ can be manipulated into the form

$$\begin{aligned}\delta\Pi=&\int_{\Omega_g}-\mathrm{div}\left\{\frac{\partial\psi_g}{\partial\mathbf{F}}\mathbf{F}^T+\left(\psi_g-\rho_g\frac{\partial\psi_g}{\partial\rho_g}\right)\mathbf{I}\right\}\cdot\delta\mathbf{u}_g+\mathrm{grad}\left\{\frac{\partial\psi_g}{\partial\rho_g}\right\}\cdot\delta\mathbf{q}\,dV+\int_{\Gamma_g}\left\{\mathbf{F}\left(\frac{\partial\psi_g}{\partial\mathbf{F}}\right)^T\right.\\&\left.+\left(\psi_g-\rho_g\frac{\partial\psi_g}{\partial\rho_g}-\psi_f+\rho_f\frac{\partial\psi_f}{\partial\rho_f}\right)\mathbf{I}\right\}\delta\mathbf{u}_g\cdot\mathbf{n}_g-\mathbf{t}\cdot\delta\mathbf{u}_g+\left\{\frac{\partial\psi_f}{\partial\rho_f}-\frac{\partial\psi_g}{\partial\rho_g}\right\}\delta\mathbf{q}\cdot\mathbf{n}_g\,dA\\&+\int_{\Omega_f}-\mathrm{grad}\left\{\psi_f-\rho_f\frac{\partial\psi_f}{\partial\rho_f}\right\}\cdot\delta\mathbf{u}_f\,dV+\int_{\Gamma_f}\left\{\psi_f-\rho_f\frac{\partial\psi_f}{\partial\rho_f}+p_{app}\right\}\delta\mathbf{u}_f\cdot\mathbf{n}_f\,dA.\end{aligned} \tag{13}$$

In the absence of constraints, the variations $\{\delta\mathbf{u}_g, \delta\mathbf{q}, \delta\mathbf{u}_f\}$ are independent and arbitrary, whereupon it follows from $\delta\Pi = 0$ that equilibrium for the swollen gel is governed by

$$\operatorname{div}\left\{\frac{\partial\psi_g}{\partial\mathbf{F}}\mathbf{F}^T + \left(\psi_g - \rho_g\frac{\partial\psi_g}{\partial\rho_g}\right)\mathbf{I}\right\} = \mathbf{0} \quad \text{in } \Omega_g, \tag{14}$$

$$\operatorname{grad}\left\{\frac{\partial\psi_g}{\partial\rho_g}\right\} = \mathbf{0} \quad \text{in } \Omega_g, \tag{15}$$

and

$$\operatorname{grad}\left\{\psi_f - \rho_f\frac{\partial\psi_f}{\partial\rho_f}\right\} = \mathbf{0} \quad \text{in } \Omega_f, \tag{16}$$

with conditions at the gel surface of

$$\left\{\mathbf{F}\left(\frac{\partial\psi_g}{\partial\mathbf{F}}\right)^T + \left(\psi_g - \rho_g\frac{\partial\psi_g}{\partial\rho_g} - \psi_f + \rho_f\frac{\partial\psi_f}{\partial\rho_f}\right)\mathbf{I}\right\}^T \mathbf{n}_g = \mathbf{t} \quad \text{on } \Gamma_g, \tag{17}$$

$$\frac{\partial\psi_g}{\partial\rho_g} = \frac{\partial\psi_f}{\partial\rho_f} \quad \text{on } \Gamma_g, \tag{18}$$

and boundary conditions on the external boundary of the fluid bath of

$$\psi_f - \rho_f\frac{\partial\psi_f}{\partial\rho_f} = -p_{app} \quad \text{on } \Gamma_f. \tag{19}$$

As stated before, these governing equations and boundary conditions have here been derived without considering the incompressibility constraint on the fluid or the volume additivity constraint on the gel. In particular, the fluid is so far regarded as compressible.

The scalar Eq. (19) would be expected to have a unique solution, which we denote by $\rho_f = \hat{\rho}_f(p_{app})$. It then follows from (16) that $\rho_f = \hat{\rho}_f(p_{app})$ throughout the fluid bath. This, in turn, permits additional simplification of the gel surface conditions (17) and (18). We collect these together with (14) and (15) to give a fully posed set of field equations and boundary conditions for the gel in the form

$$\operatorname{div}\left\{\frac{\partial\psi_g}{\partial\mathbf{F}}\mathbf{F}^T\right\} + \operatorname{grad}\left\{\psi_g - \rho_g\frac{\partial\psi_g}{\partial\rho_g}\right\} = \mathbf{0} \quad \text{in } \Omega_g, \tag{20}$$

$$\operatorname{grad}\left\{\frac{\partial\psi_g}{\partial\rho_g}\right\} = \mathbf{0} \quad \text{in } \Omega_g, \tag{21}$$

with

$$\frac{\partial\psi_g}{\partial\mathbf{F}}\mathbf{F}^T\mathbf{n}_g + \left(\psi_g - \rho_g\frac{\partial\psi_g}{\partial\rho_g}\right)\mathbf{n}_g = \mathbf{t} - p_{app}\mathbf{n}_g \quad \text{on } \Gamma_g, \tag{22}$$

$$\frac{\partial\psi_g}{\partial\rho_g} = \frac{1}{\rho_f}(p_{app} + \psi_f)\bigg|_{\rho_f = \hat{\rho}_f(p_{app})} \quad \text{on } \Gamma_g. \tag{23}$$

As discussed in detail in Baek and Srinivasa (2004a), the derivative $\partial\psi_g/\partial\rho_g$ corresponds to the chemical potential of the gel, and (21) is a requirement that this potential has zero gradient within the gel. Similarly Eq. (18), and its equivalent form (23), is a requirement that the gel chemical potential matches the bath chemical potential at the gel/bath interface.

While the set (20)–(23) applies to a gel in a compressible fluid bath, the more standard case of a gel in an incompressible fluid bath is easily obtained. For an incompressible fluid, the fluid density has constant value ρ_{f0} and the fluid free energy has constant value ψ_{f0}. As discussed in Ball and Schaeffer (1993), it was shown by Rivlin (1977) that endowing an incompressible material model with a slight degree of compressibility gives rise to a regular perturbation in the governing equations. In the present context, one may penalize fluid compressibility by introducing parameter $\varepsilon_f > 0$ and taking

$$\psi_f(\rho_f) = \psi_{f0} + \frac{(\rho_f - \rho_{f0})^2}{2\varepsilon_f}\check{\psi}_f(\rho_f, \varepsilon_f), \tag{24}$$

where the function $\check{\psi}_f$ is positive, is bounded away from zero, and has bounded derivative with respect to ρ_f. Then $\varepsilon_f \to 0^+$ describes the fluid in its incompressible limit. In this limit, one obtains the anticipated result that (20)–(22) continue to hold,

whereas (23) is replaced by

$$\frac{\partial \psi_g}{\partial \rho_g} = \frac{1}{\rho_{f0}}(p_{app} + \psi_{f0}) \quad \text{on } \Gamma_g. \tag{25}$$

The right hand side of (25) now represents the chemical potential of the incompressible fluid when it is subject to the external pressure p_{app}.

2.2. The volume additivity constraint

The governing Eqs. (20), (21) and boundary conditions (22), (25) apply to a compressible gel that is immersed in an incompressible fluid. By compressible we mean that the gel is not as yet subject to the volume additivity constraint (2). Such a theory of compressible gels would, for example, permit the existence of a void fraction at each location within the gel. In many situations, however, the volume additivity condition is met to within any reasonable measurement, and it is under these circumstances that a theory incorporating (2) has great utility (Rajagopal and Tao, 1996). In the context of porous media models that are obtained from continuum mixture theory as presented by Bowen, compressible gels are described in his 1982 paper (Bowen, 1982), whereas gels that satisfy the volume additivity constraint are described in his 1980 paper (Bowen, 1980).

For our purposes, the volume additivity constraint (2) can now be obtained by applying a limiting procedure to a suitably penalized version of the compressible theory in a fashion that is analogous to that associated with (24). Namely (viz. Baek and Srinivasa, 2004a), let $\varepsilon_g > 0$ and consider ψ_g in the form

$$\psi_g(\mathbf{F}, \rho_g) = \overline{\psi}_g(\mathbf{F}) + \frac{\phi^2}{2\varepsilon_g}\check{\psi}_g(\mathbf{F}, \rho_g, \varepsilon_g), \quad \phi \equiv \rho_g - \rho_{f0} - \frac{\rho_{s0} - \rho_{f0}}{J}, \tag{26}$$

where the function $\check{\psi}_g$ is positive, is bounded away from zero, and has bounded derivatives. Then $\varepsilon_g \to 0^+$ requires $\phi \to 0$, and hence recovers (2). One then computes for example that

$$\frac{\partial \psi_g}{\partial \mathbf{F}} = \frac{\partial \overline{\psi}_g}{\partial \mathbf{F}} + \frac{\phi}{\varepsilon_g}\left(\frac{\rho_{s0} - \rho_{f0}}{J}\right)\check{\psi}_g \mathbf{F}^{-T} + O\left(\frac{\phi^2}{\varepsilon_g}\right). \tag{27}$$

The essential feature of the limiting procedure is that $\phi \to 0$ in the same order as $\varepsilon_g \to 0^+$ so that ϕ/ε_g remains finite in the limit, whereas $\phi^2/\varepsilon_g \to 0$. Introduce

$$K_g = \lim_{\varepsilon_g \to 0^+} \frac{\phi}{\varepsilon_g}\check{\psi}_g, \tag{28}$$

which becomes indeterminate in the limit; in particular, the constitutive information resident in $\check{\psi}_g$ is not retained in the limit. Thus (27) gives

$$\frac{\partial \psi_g}{\partial \mathbf{F}} \to \frac{\partial \overline{\psi}_g}{\partial \mathbf{F}} + \left(\frac{\rho_{s0} - \rho_{f0}}{J}\right) K_g \mathbf{F}^{-T} \tag{29}$$

in this limit. In a similar fashion one finds that

$$\frac{\partial \psi_g}{\partial \rho_g} \to K_g, \quad \psi_g - \rho_g \frac{\partial \psi_g}{\partial \rho_g} \to \overline{\psi}_g - \rho_g K_g. \tag{30}$$

Now substituting from (29), (30), and using (2), one finds that (20), (21), (22), and (25) become

$$\operatorname{div}\left\{\frac{\partial \overline{\psi}_g}{\partial \mathbf{F}}\mathbf{F}^T\right\} + \operatorname{grad}\{\overline{\psi}_g - \rho_{f0} K_g\} = \mathbf{0} \quad \text{in } \Omega_g, \tag{31}$$

$$\operatorname{grad}(K_g) = \mathbf{0} \quad \text{in } \Omega_g, \tag{32}$$

with

$$\frac{\partial \overline{\psi}_g}{\partial \mathbf{F}}\mathbf{F}^T \mathbf{n}_g + (\overline{\psi}_g - \rho_{f0} K_g)\mathbf{n}_g = \mathbf{t} - p_{app}\mathbf{n}_g \quad \text{on } \Gamma_g, \tag{33}$$

$$K_g = \frac{1}{\rho_{f0}}(p_{app} + \psi_{f0}) \quad \text{on } \Gamma_g. \tag{34}$$

Inspection of the above equations shows that (32) can be used to simplify (31), and that (34) can be used to simplify (33). After making these simplifications we make a return to the notation ψ_g by making the replacement $\overline{\psi}_g(\mathbf{F}) \to \psi_g(\mathbf{F})$. The result is that (31) and (33) become

$$\operatorname{div}\left\{\frac{\partial \psi_g}{\partial \mathbf{F}}\mathbf{F}^T + \psi_g \mathbf{I}\right\} = \mathbf{0} \quad \text{in } \Omega_g, \tag{35}$$

$$\left\{\frac{\partial\psi_g}{\partial\mathbf{F}}\mathbf{F}^T+(\psi_g-\psi_{f0})\mathbf{I}\right\}\mathbf{n}_g=\mathbf{t}\quad\text{on }\Gamma_g. \tag{36}$$

It is significant to note that neither K_g nor the pressure p_{app} of the surrounding fluid appear in the set (35) and (36). As discussed in Baek and Srinivasa (2004a), K_g corresponds to the chemical potential of the gel, which, as the above procedure shows, no longer has an essential role when incorporating the constraint (2). In fact, even though K_g is no longer essential, Eqs. (32) and (34) formally give that $K_g=(p_{app}+\psi_{f0})/\rho_{f0}$ throughout Ω_g. Such a state of affairs is not unusual. Namely, when a kinematical descriptor is no longer independent, as is the case of ρ_g under (2), then its work conjugate kinetic quantity, here K_g, satisfies its appropriate balance principle a-priori in a manner that is independent of the constitutive theory (viz. Gurtin, 2000).

Let us now assume that the total free energy of the swollen polymer can be written in the form

$$\psi_g(\mathbf{F})=\frac{1}{J}(\Psi(\mathbf{F})+H(J))+\left(1-\frac{1}{J}\right)\psi_{f0}, \tag{37}$$

where $\Psi(\mathbf{F})$ and $H(J)$ represent the free energies due to polymer deformation and polymer-fluid mixing, respectively. It is then convenient to define the new energy function

$$W(\mathbf{F})=\Psi(\mathbf{F})+H(J). \tag{38}$$

In terms of this $W=W(\mathbf{F})$ the governing equation for the gel (35) and its accompanying boundary condition (36) become simply

$$\operatorname{div}\left\{\frac{1}{J}\frac{\partial W}{\partial\mathbf{F}}\mathbf{F}^T\right\}=\mathbf{0}\quad\text{in }\Omega_g, \tag{39}$$

$$\left\{\frac{1}{J}\frac{\partial W}{\partial\mathbf{F}}\mathbf{F}^T\right\}\mathbf{n}_g=\mathbf{t}\quad\text{in }\Gamma_g. \tag{40}$$

The form of these equations is exactly that which applies to a compressible hyperelastic solid with stored energy density W. This correspondence was remarked upon by Treloar (1975). For a fluid saturated gel polymer, this "apparent compressibility" is a consequence of the fact that a fixed amount of polymer can be associated with a variable amount of fluid. Eqs. (38)–(40) also form the basis for treating the equilibrium of saturated gels in Deng and Pence (2010a,b).

The form of W as given by (38) indicates that physical considerations giving rise to any proposed form of W should not account for the underlying free energy of the base fluid within the gel, i.e., energy stored in the fluid that does not arise from interaction with the polymer component is not to be included in W. Instead W should only account for the free energy of the deforming polymer, along with free energy terms associated with interactions between the polymer and fluid components of the gel. In addition, comparing (37) with (38) we note the absence of the multiplier $1/J$ in (38). This can be viewed as scaling the energy function W so that it is an energy density with respect to polymer volume in the reference configuration, which is again consistent with the formulation of compressible hyperelasticity. Constitutive forms for energy functions appropriate for polymeric gels can be obtained for example from Treloar (1975), Wineman and Rajagopal (1992), Baek and Srinivasa (2004a,b), Deng and Pence (2010a). Later in this paper when we turn to specific examples we shall consider a standard form for W in (38) which takes a neo-Hookean form for Ψ and the Flory–Huggins form for H, namely

$$\Psi=\frac{\mu}{2}(\mathbf{F}:\mathbf{F})=\frac{\mu}{2}(\mathbf{C}:\mathbf{I}),\quad H(J)=M((J-1)\ln(1-J^{-1})+\chi(1-J^{-1})), \tag{41}$$

where μ, M, and χ are constitutive parameters whose physical significance is discussed for example in Wineman and Rajagopal (1992), Deng and Pence (2010a).

3. Interactions with a vapor phase and loss of saturation

The volume additivity constraint as considered in the previous section was developed in the context of a fluid saturated gel that is surrounded by a bath of the pure fluid. The pure fluid itself was taken to be incompressible. One could alternatively consider the case where the saturated gel is removed from this fluid bath and is instead placed in an environment where it makes direct contact with a gaseous phase consisting of the gel fluid in vapor form. Here we consider modifications to the previous treatment to address such vapor phase interactions. It is the vapor phase that is now subject to the pressure load p_{app}. It will be assumed that the fluid within the gel can still be regarded as being in the liquid form. In other words the gel is still a solid–fluid mixture as opposed to a solid–gas mixture. The liquid within the gel is still regarded as incompressible when in its fluid form. We also wish to consider gels that obey the volume additivity constraint. For simplicity, the gaseous phase is treated as consisting of a gas of a pure vapor of the same liquid that constitutes the gel.

3.1. A gel in direct contact with the vapor phase

To obtain governing equations and boundary conditions, it is again useful to start by considering a gel whose external boundary is in contact with a surrounding media, where the gel and media are not constrained by notions of incompressibility

and volume additivity. This was in fact the situation considered in the previous section, where the variational procedure eventually led to (20)–(23). Eqs. (20)–(23) also serve as the starting point for the consideration of vapor phase interactions. The main difference between the treatment of this section with that of the previous section is due to the compressibility of the vapor phase. Thus we do not invoke the limiting process associated with (24) that in turn led to (25). We do, however, wish to invoke the limiting process associated with (26) as $\varepsilon_g \to 0^+$. In this way we consider a gel that is subject to the volume additivity constraint (2) while being in contact with a vapor phase instead of being in contact with an incompressible fluid bath.

In order to emphasize this new state of affairs we shall use notation ρ_v for the vapor density, and $\psi_v = \psi_v(\rho_v)$ for the free energy of the gas phase. We also write Ω_v and Γ_v in place of Ω_f and Γ_f. It is then the case that the pressure in the gas is determined by equations analogous to (16) and (19), namely

$$\operatorname{grad}\left\{\psi_v - \rho_v \frac{\partial \psi_v}{\partial \rho_v}\right\} = \mathbf{0} \quad \text{in } \Omega_v, \tag{42}$$

and

$$\psi_v - \rho_v \frac{\partial \psi_v}{\partial \rho_v} = -p_{app} \quad \text{on } \Gamma_v. \tag{43}$$

It is again assumed that the latter equation has a unique solution which defines the function $\hat{\rho}_v(p_{app})$ that gives the density of the gas as a function of the pressure. It then follows from (42) that $\rho_v = \hat{\rho}_v(p_{app})$ throughout the vapor domain Ω_v. Eqs. (20)–(22) are unchanged, while (23) is simply rewritten with new subscripts as

$$\frac{\partial \psi_g}{\partial \rho_g} = \frac{1}{\rho_v}(p_{app} + \psi_v)\Big|_{\rho_v = \hat{\rho}_v(p_{app})} \quad \text{on } \Gamma_g. \tag{44}$$

The constraint of volume additivity is now enforced by a limiting procedure that is formally identical to that associated with (26)–(30). By this means, one again eliminates K_g as defined in (28) so as to arrive at

$$\operatorname{div}\left\{\frac{\partial \psi_g}{\partial \mathbf{F}}\mathbf{F}^T + \psi_g \mathbf{I}\right\} = \mathbf{0} \quad \text{in } \Omega_g, \tag{45}$$

$$\left\{\frac{\partial \psi_g}{\partial \mathbf{F}}\mathbf{F}^T + (\psi_g - \psi_{f0})\mathbf{I}\right\}\mathbf{n}_g = \mathbf{t} + \left[\left(\frac{\rho_{f0}}{\rho_v} - 1\right)p_{app} + \frac{\rho_{f0}}{\rho_v}\psi_v - \psi_{f0}\right]\Big|_{\rho_v = \hat{\rho}_v(p_{app})}\mathbf{n}_g \quad \text{on } \Gamma_g. \tag{46}$$

These equations are to be compared with the previous set (35), (36) which applied to a gel in contact with a liquid bath. Here it is to be noted that the governing Eqs. (35) and (45) are the same, whereas the boundary conditions (36) and (46) are different. In particular, the boundary condition (46) is now influenced by both the external pressure p_{app} and by the vapor free energy ψ_v.

In view of (43) it is to be noted that (46) can also be rewritten as

$$\left\{\frac{\partial \psi_g}{\partial \mathbf{F}}\mathbf{F}^T + (\psi_g - \psi_{f0})\mathbf{I}\right\}\mathbf{n}_g = \mathbf{t} + \left[\left(\rho_{f0}\frac{\partial \psi_v}{\partial \rho_v} - \psi_{f0}\right) - \left(\rho_v \frac{\partial \psi_v}{\partial \rho_v} - \psi_v\right)\right]\Big|_{\rho_v = \hat{\rho}_v(p_{app})}\mathbf{n}_g \quad \text{on } \Gamma_g. \tag{47}$$

As an aside, it follows that formally taking $\rho_v = \rho_{f0}$ and $\psi_v = \psi_{f0}$ in (47) now retrieves (36). Note therefore that a limiting process akin to that associated with a modified form of (24), namely $\psi_v(\rho_v) = \psi_{f0} + (\rho_v - \rho_{f0})^2 \check{\psi}_v(\rho_v, \varepsilon_v)/2\varepsilon_v$ in the limit $\varepsilon_v \to 0^+$, will make $\rho_v \to \rho_{f0}$ and $\psi_v \to \psi_{f0}$. One therefore concludes, from a strictly mathematical point of view, that the order of the limiting processes associated with incompressibility of the material comprising the bath and volume additivity in the gel does not affect the final outcome. In other words governing Eqs. (35) and (36) are obtained provided that both limiting processes are considered irrespective of the order in which they are conducted.

However, for our present consideration of a gel in direct contact with a vapor phase, the bath is regarded as compressible and we have obtained governing equations (45) with gel boundary conditions (46). In terms of the free energy W defined via (37) and (38) one thus obtains

$$\operatorname{div}\left\{\frac{1}{J}\frac{\partial W}{\partial \mathbf{F}}\mathbf{F}^T\right\} = \mathbf{0} \quad \text{in } \Omega_g, \tag{48}$$

$$\left\{\frac{1}{J}\frac{\partial W}{\partial \mathbf{F}}\mathbf{F}^T\right\}\mathbf{n}_g = \mathbf{t} + \left[\left(\frac{\rho_{f0}}{\rho_v} - 1\right)p_{app} + \frac{\rho_{f0}}{\rho_v}\psi_v - \psi_{f0}\right]\Big|_{\rho_v = \hat{\rho}_v(p_{app})}\mathbf{n}_g \quad \text{on } \Gamma_g. \tag{49}$$

3.2. Loss of saturation

The equilibrium states described in the preceding section are, for a given constitutive description, determined by the loading variables $\mathbf{t}$ and p_{app}. Subsequent changes to either $\mathbf{t}$ or p_{app} would disrupt this equilibrium state and give rise to complicated non-equilibrium processes before the new equilibrium state associated with the changed $\mathbf{t}$ and p_{app} is attained. This new equilibrium is attained only after these processes have come to rest. In general there would be a variety of time

scales associated with these non-equilibrium processes. Time scales associated with stress equilibration within the solid component of the gel would generally be much shorter than time scales associated with fluid migration within the gel. For the various gel scenarios discussed thus far, one could generally estimate the various time scales and so identify, in each case, the slowest non-equilibrium process.

Consider the case of a gel that is directly in contact with the vapor phase. The various non-equilibrium process would then consist of stress wave propagation in the solid and fluid components of the gel, fluid seepage within the gel, evaporation and condensation at the gel surface, pressure wave transit in the vapor, and motion of the vapor component. Each has its characteristic time scale, and it would often be the case that the slowest time scale would be that associated with evaporation and condensation processes at the gel surface. In addition, there is a loading time scale associated with changes in $\mathbf{t}$ and p_{app}.

In this context, let us consider the case where the evaporation and condensation time scale is much longer than all other time scales. Changes in loading then lead to a situation where the other physical processes: stress and pressure wave propagation, fluid seepage, gas motion, etc., all essentially come to rest with respect to the current, slowly changing, mass distribution at the gel's interface with the vapor phase. As mass is transferred across this surface, these other processes are regarded as giving rise to equilibrated stress and chemical potential fields within the gel, even though mass transfer is proceeding at the gel surface, albeit it at a time scale that is much longer than all other time scales in the problem.

To describe this state of affairs at the faster time scales of interest, one may consider a treatment in which there is no transfer of the gel's liquid component across the gel surface. Prior to the imposition of any constraints, the variational procedure is still $\delta\Pi = 0$ with

$$\delta\Pi = \delta\left(\int_{\Omega_g}\psi_g dV + \int_{\Omega_v}\psi_v\, dV\right) - \int_{\Gamma_g}\mathbf{t}\cdot\delta\mathbf{u}_g\, dA + \int_{\Gamma_v} p_{app}\mathbf{n}_v\cdot\delta\mathbf{u}_f\, dA, \tag{50}$$

for all admissible variations $\{\delta\mathbf{u}_g, \delta\mathbf{q}, \delta\mathbf{u}_v\}$. One then obtains

$$\delta\left(\int_{\Omega_g}\psi_g dV + \int_{\Omega_v}\psi_v\, dV\right) = \int_{\Omega_g}\delta\psi_g dV + \int_{\Gamma_g}(\psi_g - \psi_v)\delta\mathbf{u}_g\cdot\mathbf{n}_g\, dA + \int_{\Omega_v}\delta\psi_v\, dV + \int_{\Gamma_v}\psi_v\delta\mathbf{u}_v\cdot\mathbf{n}_v\, dA, \tag{51}$$

and we observe that (50) and (51) could be obtained directly from (6) and (7) by replacing all subscripts f with subscript v. In a similar fashion (3), (4), (5), (8), (10), (11), and (12) continue to hold under this same subscript replacement. We are therefore led to an expression for $\delta\Pi$ that is given by (13) provided that subscripts f become subscript v. In this setting we consider the case in which there is no liquid flux through the gel interface Γ_g. Thus the variation $\delta\mathbf{q}$ is subject to the condition $\delta\mathbf{q}\cdot\mathbf{n}_g = \mathbf{0}$ on Γ_g. In view of the $f\to v$ analogue of (3) this is equivalent to the kinematic constraint $\delta\mathbf{u}_g\cdot\mathbf{n}_g = \delta\mathbf{u}_v\cdot\mathbf{n}_g$ on Γ_g on the displacement variations.

In extracting governing equations from the variational requirement $\delta\Pi = 0$ it follows that the multiplier of $\delta\mathbf{q}\cdot\mathbf{n}_g$ on Γ_g is no longer required to vanish. Thus by the same reasoning as that used in the first paragraph of Section 3.1 it is concluded that $\rho_v = \hat{\rho}_v(p_{app})$ throughout Ω_v and that the gel is subject to governing Eqs. (20) and (21) on Ω_g, and boundary condition (22) on Γ_g. However, the other boundary condition on Γ_g, namely (44) which derived from (19) under $f\to v$, is no longer required to hold. Instead it is replaced by the kinematic condition of no mass transfer through the gel boundary Γ_g prior to reestablishment of equilibrium within the gel. This gives that

$$M_* = \int_{\Omega_g}\rho_g\, dV = \int_{\Omega_{g_{\mathbf{X}}}}\rho_g J\, dV_{\mathbf{X}}, \tag{52}$$

where M_* is the now fixed total mass within the gel. The second integral in (52) is taken as over the reference volume of the gel, which is why we use the notation $\Omega_{g_{\mathbf{X}}}$ and $dV_{\mathbf{X}}$ in the second integral expression.

We now impose the constraint of volume additivity (2) within the gel while still treating the vapor as compressible. This is the same procedure that led to (45) and (46) when condition (44) was operative. This again leads to (45). However now, because (44) no longer applies, one does not obtain the condition (46) on Γ_g. Instead of (46) one obtains

$$\left\{\frac{\partial\psi_g}{\partial\mathbf{F}}\mathbf{F}^T + (\psi_g - \psi_{f0})\mathbf{I}\right\}\mathbf{n}_g = \mathbf{t} + \left[(\rho_{f0}K_g - \psi_{f0}) - \left(\rho_v\frac{\partial\psi_v}{\partial\rho_v} - \psi_v\right)\right]\Big|_{\rho_v = \hat{\rho}_v(p_{app})}\mathbf{n}_g \quad \text{on } \Gamma_g, \tag{53}$$

where K_g is again as defined in (28). It is to be remarked that this K_g is spatially constant since the limiting process again gives (32). All of the other variables appearing within the brackets of (53) are also independent of location on Γ_g. Thus the bracketted expression within (53) is constant on Γ_g, although its value is so far arbitrary since it contains K_g. It is therefore convenient to define a new arbitrary constant

$$P = \left[(\rho_{f0}K_g - \psi_{f0}) - \left(\rho_v\frac{\partial\psi_v}{\partial\rho_v} - \psi_v\right)\right]\Big|_{\rho_v = \hat{\rho}_v(p_{app})} \tag{54}$$

so that (53) can be written

$$\left\{\frac{\partial\psi_g}{\partial\mathbf{F}}\mathbf{F}^T + (\psi_g - \psi_{f0})\mathbf{I} - P\mathbf{I}\right\}\mathbf{n}_g = \mathbf{t} \quad \text{on } \Gamma_g. \tag{55}$$

In addition, in terms of the free energy W defined via (37) and (38) one now obtains from (45) and (55) that

$$\mathrm{div}\left\{\frac{1}{J}\frac{\partial W}{\partial \mathbf{F}}\mathbf{F}^T\right\}=\mathbf{0} \quad \text{in } \Omega_g, \tag{56}$$

$$\left\{\frac{1}{J}\frac{\partial W}{\partial \mathbf{F}}\mathbf{F}^T-P\right\}\mathbf{n}_g=\mathbf{t} \quad \text{on } \Gamma_g. \tag{57}$$

We may now also simplify the mass conservation condition (52) by using (2) so as to obtain

$$M_*=\int_{\Omega_{g_\mathbf{X}}}\rho_g J\,dV_\mathbf{X}=\int_{\Omega_{g_\mathbf{X}}}(\rho_{s0}+(J-1)\rho_{f0})\,dV_\mathbf{X}. \tag{58}$$

Introduce the dry volume of the polymeric constituent

$$V_p=\int_{\Omega_{g_\mathbf{X}}}dV_\mathbf{X}, \tag{59}$$

whereupon (58) finally gives

$$\int_{\Omega_{g_\mathbf{X}}}J\,dV_\mathbf{X}=V_*, \tag{60}$$

where

$$V_*=\frac{1}{\rho_{f0}}(M_*-(\rho_{s0}-\rho_{f0})V_p) \tag{61}$$

is the fixed total volume of the unsaturated gel. Eqs. (56), (57), and (60) are equivalent to those employed in Deng and Pence (2010a,b) for the description of equilibrium deformations of unsaturated gels.

3.3. Recapitulation

Table 1 summarize various gel scenarios described in this and the previous section. All of the cases listed in the table correspond to a gel in which the constraint (2) holds throughout the gel. Alternatively the field equations and gel surface conditions can be expressed as

$$\mathrm{div}\boldsymbol{\sigma}=\mathbf{0} \text{ in } \Omega_g, \quad \boldsymbol{\sigma}\mathbf{n}_g=\mathbf{t} \text{ in } \Gamma_g, \tag{62}$$

where the stress tensor $\boldsymbol{\sigma}$ is given by

$$\boldsymbol{\sigma}=\frac{2}{J}\mathbf{F}\frac{\partial W}{\partial \mathbf{C}}\mathbf{F}^T+\begin{cases}0\mathbf{I} & \text{if saturated,}\\ -P\mathbf{I} & \text{if unsaturated,}\\ -\left[\left(\dfrac{\rho_{f0}}{\rho_v}-1\right)p_{app}+\dfrac{\rho_{f0}}{\rho_v}\psi_v-\psi_{f0}\right]\mathbf{I}\Big|_{\rho_v=\hat{\rho}_v(p_{app})} & \text{if equilibrated with vapor.}\end{cases} \tag{63}$$

Here the objectivity condition $W=W(\mathbf{C})$ is used in (63). Note also that the final multipliers of the identity tensor $\mathbf{I}$ are constant for each of these three scenarios.

In view of these different gel scenarios let us consider again load induced loss-of-saturation. Specific examples of loss of saturation were examined in Deng and Pence (2010a,b). The loss-of-saturation transition corresponds to the governing Eqs. {(39), (40)} changing to governing Eqs. {(56), (57), (60)} at the instant when the last bit of liquid is imbibed by the gel. As our focus is restricted exclusively to equilibrium states, it is assumed therefore that the change in load $\mathbf{t}$ – which is driving the process – takes place sufficiently slowly so that the various dynamical phenomena described earlier come to rest on time scales that are much shorter than that of the change in load. In particular, the present treatment does not apply at shorter time scales when such dynamical processes are active (such as the liquid diffusion within the gel). At the instant that saturation is lost, the value of P is initially zero because the final saturated state determines V_* and so, by definition, satisfies the global constraint (60). Additional change in $\mathbf{t}$ that increases the amount of undersaturation gives rise to a nonzero P with changes in P correlating to changes in $\mathbf{t}$ in a continuous manner. This in turn accounts for the stiffer response of the unsaturated gel. Indeed

Table 1
Governing equations for different types of systems.

Situation	Surrounded by	Gel boundary variation	Field equation	Gel surface condition	Side condition
Saturated	Liquid (incompressible)	(3)	(39)	(40)	None
Unsaturated	Vapor (compressible)	$\delta\mathbf{q}\cdot\mathbf{n}_g=\mathbf{0}$	(56)	(57)	(60)
Equilibrated with vapor	Vapor (compressible)	(3)	(48)	(49)	None

P can be viewed as an all-around constant hydrostatic pressure that drives out just the right amount of liquid from a hypothetical saturated gel so as to make the overall liquid content consistent with the constraint (60).

In one respect, however, the process as described in the previous paragraph is not a sequence of equilibrium states. This is because the mass transfer at the gel surface by evaporation/condensation is regarded as taking place on a time scale that is even slower than that of the changing load $\mathbf{t}$. On time scales that are on the order of the evaporative time scale, equilibrium is described mathematically by means of (48), (49). Consider therefore the following loading process. The gel first undergoes loss-of-saturation by virtue of surface tractions $\mathbf{t}$ that are, at first, changing slowly with respect to all time scales except that of evaporation which operates on an even longer time scale. Then, later, $\mathbf{t}$ is subsequently held fixed for all future time. Prior to $\mathbf{t}$ being held fixed the system is modeled on the basis of (56), (57), (60). For sufficiently large time, however, the system is modeled on the basis of (48), (49). Formally, (49) from the latter set is obtained from (57) of the former set by assigning to K_g the value of $\partial\psi_v/\partial\rho_v$ given in Eq. (54). Thus the transition from the unsaturated treatment in the second line of the Table to the fully equilibrated treatment of the third line of the Table can be viewed as described by the value of K_g changing from its constraint value as determined by (60) – which makes this initial K_g independent of vapor properties – to the value $\partial\psi_v/\partial\rho_v$ which is the chemical potential of the vapor phase.

The determination of complicated states of deformation for any of the situations indicated in Table 1 motivates the consideration of finite element methods. Accordingly, new constitutive models are often implemented using a user-supplied subroutine in commercial FEM software. Recently, for example, a variety of inhomogeneous deformation solutions corresponding to a swollen saturated gel were obtained with the aid of ABACUS by Hong et al. (2009). Developing such a user-supplied subroutine in the context of a commercial software package presents its own issues, one of which is that it is not always clear that such an implementation–even if possible with regard to current modeling–will be consistent with an easy route for continued modification so as to incorporate future modeling advances. This motivates us to develop from scratch both 2D axisymmetric and 3D FEM codes using Matlab so as to describe these states of gel equilibrium. We now describe the essential features of such algorithms and then demonstrate their efficacy in analyzing inhomogeneous deformation of a swollen gel.

4. Application: Modeling of an everted swollen tube

As demonstration we consider equilibrium deformations corresponding to the axisymmetric eversion of a cylindrical gel tube, meaning that the tube is turned inside-out. This is easily accomplished for example in short pieces of rubber hosing. The eversion deformation has a long history of study in conventional hyperelasticity beginning with Rivlin in the context of the incompressible theory (Rivlin, 1949) and then leading through more recent work (Haughton and Orr, 1997, 1996; Chen and Haughton, 1997) in the context of the compressible theory. The case of tubes composed of polymer gels, which for saturated gels corresponds to the compressible theory with W given by (41), was examined in Deng and Pence (2010a). That work also examined aspects of the eversion deformation for an unsaturated gel.

Let $\Omega_{g_\mathbf{x}}$ be the domain of the initially dry polymer body $\mathcal{B}$ in the reference configuration. The position of a particle in $\Omega_{g_\mathbf{x}}$ is denoted by $\mathbf{X}_g=\hat{\mathbf{X}}_g(R^s,\Theta^s,Z^s)$ in a cylindrical coordinate system with

$$R_i^s\le R^s\le R_o^s,\quad 0\le\Theta^s<2\pi,\quad -L^s\le Z^s\le 0. \tag{64}$$

The swollen and deformed body $\kappa(\mathcal{B})$ occupies domain Ω_g with particle positions denoted by $\mathbf{x}=\hat{\mathbf{x}}(r,\theta,z)$. General axisymmetric eversion deformations are then of the form $r=\tilde{r}(R^s,Z^s)$, $\theta=\Theta^s$, and $z=\tilde{z}(R^s,Z^s)$ where $\partial\tilde{r}/\partial R^s<0$.

In Deng and Pence (2010a) it is the special case $\tilde{r}=\tilde{r}(R^s)$ and $\tilde{z}=-\lambda_z Z^s$, where $\lambda_z>0$ is a constant, that is studied in detail. The inherent simplification of this special case reduces boundary value problems to the consideration of ordinary differential equations. These simplifications are generally not consistent with zero tractions at each point on the external boundary. Specifically, to obtain equilibrium deformations of such a simplified form it is necessary to impose the normal displacement on the tube caps (the surfaces that were $Z^s=-L^s$ and $Z^s=0$ in the reference configuration). On the other hand, if one seeks equilibrium solutions corresponding to a completely released and everted tube (i.e., zero tractions on *all* external surfaces) then one must consider deformations with the more general function dependence $r=\tilde{r}(R^s,Z^s)$ and $z=\tilde{z}(R^s,Z^s)$. Such deformations are not treatable by the method of ordinary differential equations given in Deng and Pence (2010a). This is what accounts for their consideration here in the context of more general finite element methods. To this end the overall mapping $(R^s,\Theta^s,Z^s)\to(r,\theta,z)$ will be decomposed into a suite of three separate mappings:

- A free swelling mapping $(R^s,\Theta^s,Z^s)\to(R^{fs},\Theta^{fs},Z^{fs})$.
- A mapping to a convenient computational domain $(R^{fs},\Theta^{fs},Z^{fs})\to(R,\Theta,Z)$.
- The mapping to the final deformed configuration $(R,\Theta,Z)\to(r,\theta,z)$.

We represent this decomposition as $\mathcal{B}\to\kappa^{fs}(\mathcal{B})\to\kappa^R(\mathcal{B})\to\kappa(\mathcal{B})$ and now describe each mapping in turn.

After immersing the initially dry polymer into the liquid, the resulting gel gradually swells and reaches an equilibrium state in the absence of external loading. If sufficient fluid is available to saturate the polymer then the gel is said to be freely swollen. The freely swollen gel then occupies a new domain Ω_g^{fs} and this deformation is described in a cylindrical coordinate system as

$$R^{fs}=\zeta R^s,\quad \Theta^{fs}=\Theta^s,\quad Z^{fs}=\zeta Z^s, \tag{65}$$

where $\zeta > 1$ is the free swelling ratio. Under free swelling the inner radius and outer radius become ζR_i^s and ζR_o^s, respectively. The free swelling deformation gradient is $\mathbf{F}^{fs} = \zeta\mathbf{I}$ whereupon it follows that ζ can be found from $W(\mathbf{F})$ by requiring that

$$\frac{d}{d\zeta} W(\zeta\mathbf{I}) = 0. \tag{66}$$

For $W(\mathbf{F}) = \Psi(\mathbf{F}) + H(J)$ in the form (41) this gives

$$\ln(1-\zeta^{-3}) + \zeta^{-3} + \chi\zeta^{-6} + \frac{\mu}{M}\zeta^{-1} = 0, \tag{67}$$

which is one form of the Flory–Huggins equation. Even if there is insufficient liquid to freely swell the body, we continue to use the mapping (65) in the ensuing development.

Now the swollen cylinder is everted by applying external tractions sufficient to turn the tube inside-out. Releasing the tube may or may not cause the tube to pop back to its original shape depending on material properties and tube dimensions. If the tube remains everted then it again slowly reaches a new equilibrium under the influence of various dynamical process such as fluid migration within the gel. Alternatively, the eversion process may take place sufficiently slowly so as to proceed through what is essentially a sequence of equilibrium states. Either way, the deformed equilibrium shape of the fully released everted tube $\kappa(\mathcal{B})$ will no longer be that of a perfect cylinder due to residual stress.

The direct mapping $\kappa^{fs}(\mathcal{B}) \to \kappa(\mathcal{B})$ would introduce extreme distortions to finite elements defined directly on $\kappa^{fs}(\mathcal{B})$. This is avoided by considering the configuration $\kappa^R(\mathcal{B})$ that has the shape of a perfect cylinder with domain Ω_R where the associated particle positions $\mathbf{X} = \hat{\mathbf{X}}(R,\Theta,Z)$ are mapped from $\mathbf{\Omega}_g^{fs}$ by

$$R = -R^{fs} + \zeta R_i^s + \zeta R_o^s, \quad \Theta = \Theta^{fs}, \quad Z = -Z^{fs}. \tag{68}$$

Since $\partial R/\partial R^{fs} < 0$ this mapping $\kappa^{fs}(\mathcal{B}) \to \kappa^R(\mathcal{B})$ represents an extremely simple eversion. In what follows we shall make use of the notation $R_o \overset{\text{def}}{=} \zeta R_i^s$ and $R_i \overset{\text{def}}{=} \zeta R_o^s$ which acknowledges that the eversion maps particles that were originally on the inner radius to the outer radius and vice-versa. In general, stresses computed in the body $\kappa^R(\mathcal{B})$ would not satisfy $(62)_1$ and so such a state would require not only the application of surface tractions, but also the application of body forces. This is, however, not relevant for our purposes since $\kappa^R(\mathcal{B})$ here serves as a convenient hypothetical configuration on which to define finite elements. After the final mapping $\kappa^R(\mathcal{B}) \to \kappa(\mathcal{B})$, all stresses in $\kappa(\mathcal{B})$ will satisfy finite element equations associated with Eq. (62) of the theoretical development. The position of the particle in the current (deformed) configuration is denoted by $\mathbf{x} = \hat{\mathbf{x}}(r,\theta,z)$ and the mapping $\kappa^R(\mathcal{B}) \to \kappa(\mathcal{B})$ is the axisymmetric deformation given by

$$r = \hat{r}(R,Z), \quad \theta = \Theta, \quad z = \hat{z}(R,Z). \tag{69}$$

It is this mapping which is determined by the finite element procedure.

At this point in the development we amend our notation so as to replace $\mathbf{F}$ in all previous sections by the notation $\mathbf{F}_{g_\mathbf{x}}$. In the present example of the eversion deformation, $\mathbf{F}_{g_\mathbf{x}}$ represents the deformation gradient associated with the full deformation mapping $\mathcal{B} \to \kappa(\mathcal{B})$. This replacement is made so as to now use the notation $\mathbf{F}$ for the deformation gradient associated with the mapping (69) which is to be obtained directly by the finite element procedure. In view of the three mappings (65), (68), and (69) – that together comprise the deformation from the nominally dry reference configuration of the polymer constituent to that of the swollen, everted gel cylinder – we write

$$\mathbf{F}_{g_\mathbf{x}} = \mathbf{F}\mathbf{F}^R\mathbf{F}^{fs}, \tag{70}$$

where $\mathbf{F}^{fs} = \zeta\mathbf{I}$,

$$\mathbf{F}^R = \begin{bmatrix} -1 & 0 & 0 \\ 0 & \left[\frac{R_o+R_i}{R} - 1\right]^{-1} & 0 \\ 0 & 0 & -1 \end{bmatrix}, \quad \text{and} \quad \mathbf{F} = \begin{bmatrix} \frac{\partial \hat{r}}{\partial R} & 0 & \frac{\partial \hat{r}}{\partial Z} \\ 0 & \frac{\hat{r}}{R} & 0 \\ \frac{\partial \hat{z}}{\partial R} & 0 & \frac{\partial \hat{z}}{\partial Z} \end{bmatrix}. \tag{71}$$

In the above expression for $\mathbf{F}^R$ we recall that $R_o = \zeta R_i^s$ and $R_i = \zeta R_o^s$.

In what follows it is convenient to consider $\mathbf{F}^s \overset{\text{def}}{=} \mathbf{F}^R\mathbf{F}^{fs}$ which can be considered as a tensorial quantity representing the pre-stretch of the body in the computational domain Ω_R. It is written from (71) as

$$\mathbf{F}^s = \begin{bmatrix} -\zeta & 0 & 0 \\ 0 & \zeta\left[\frac{R_o+R_i}{R} - 1\right]^{-1} & 0 \\ 0 & 0 & -\zeta \end{bmatrix}. \tag{72}$$

In Sections 2 and 3, it has been shown that the form of the equilibrium equation under a static loading condition is exactly that which applies to a compressible hyperelastic solid with stored energy density W. Thus, we model the quasi-static behavior of the swollen polymer as a compressible material whose stored energy density (per unit volume in $\Omega_{g_\mathbf{x}}$) is given by a function of the right Cauchy–Green tensor $\mathbf{C}_{g_\mathbf{x}} = \mathbf{F}_{g_\mathbf{x}}^T\mathbf{F}_{g_\mathbf{x}}$. Specifically, we take this stored energy in the form (38), i.e., $W(\mathbf{C}_{g_\mathbf{x}}) = \Psi(\mathbf{C}_{g_\mathbf{x}}) + H(J_{g_\mathbf{x}})$ where, henceforth, Ψ and H are given by (41).

Since a nominally pre-stressed configuration $\kappa^R(\mathcal{B})$ is used as the computational domain Ω_R, it is convenient to reformulate the constitutive relation with respect to $\kappa^R(\mathcal{B})$. It is similarly convenient to make use of standard indicial notation to present

the ensuing finite element equations. For example, the stress $\boldsymbol{\sigma}$ in (63) for a saturated gel would now be written as

$$\boldsymbol{\sigma} = \frac{2}{J_{g\mathbf{x}}}\mathbf{F}_{g\mathbf{x}}\frac{\partial W(\mathbf{C}_{g\mathbf{x}})}{\partial \mathbf{C}_{g\mathbf{x}}}\mathbf{F}_{g\mathbf{x}}^T. \tag{73}$$

However, using a push-forward operation, the stress $\boldsymbol{\sigma}$ in (73) is now written with respect to $\kappa^R(\mathcal{B})$ as

$$\boldsymbol{\sigma} = \frac{2}{J}\mathbf{F}\frac{\partial \hat{W}(\mathbf{C})}{\partial \mathbf{C}}\mathbf{F}^T \quad \text{with } \hat{W}(\mathbf{C}) = \frac{1}{J^s}W((\mathbf{F}^s)^T\mathbf{C}\mathbf{F}^s), \tag{74}$$

where $J=\det \mathbf{F}$ and $J^s=\det \mathbf{F}^s$. The "known" quantities $\mathbf{C}^s$ and J^s are suppressed in the notation $\hat{W}(\mathbf{C})$. By virtue of (38) and (41) this gives $\hat{W}(\mathbf{C}) = \hat{\Psi}(\mathbf{C}) + \hat{H}(J)$ where

$$\hat{\Psi}(\mathbf{C}) = \frac{\mu}{2J^s}(F^s_{\alpha i}F^s_{\beta i}C_{\alpha\beta} - 3),$$

$$\hat{H}(J) = \frac{M}{J^s}\left[(J^sJ-1)\ln\left(1-\frac{1}{J^sJ}\right) + \chi\left(1-\frac{1}{J^sJ}\right)\right], \tag{75}$$

and μ, M, and χ are again the material parameters. The local volume change from the solid state can also be calculated by $J_{g\mathbf{x}}=JJ^s$.

5. Finite element formulation

A weak form for a saturated gel can be obtained by finding $\mathbf{x}$ which satisfies the following equation for all admissible $\delta\mathbf{x}$,

$$\delta\Pi = \int_{\Omega_R}\frac{\partial \hat{\Psi}}{\partial \mathbf{C}} : \delta\mathbf{C} + \hat{H}'(J)\frac{\partial J}{\partial \mathbf{C}} : \delta\mathbf{C}\, dV - \int_{\Gamma_t}\mathbf{t}\cdot\delta\mathbf{x}\, da = 0, \tag{76}$$

where the last term represents the work done by the traction $\mathbf{t}$ on the boundary Γ_t in the current configuration. Using $\mathbf{n}da = J\mathbf{F}^{-T}\mathbf{N}\, dA$ and defining $\mathbf{t}^o = J\mathbf{T}\mathbf{F}^{-T}\mathbf{N}$ on Γ_R (the inverse image of Γ_t on the boundary of Ω_R) this surface integral can be rewritten with respect to the computational domain as $\int_{\Gamma_R}\mathbf{t}^o\cdot\delta\mathbf{x}dA$. To solve various boundary value problems, we present both a 2D FEM for axisymmetric loading and a 3D FEM for more general problems.

5.1. FE formulation for an axisymmetric deformation

The axisymmetric FEM for (76) involves approximating the current position $\mathbf{x}=\{r(R,Z), z(R,Z)\}$ in a triangular element by

$$x_i = \Phi_{iB}x_B^p, \tag{77}$$

where $x_B^p=[r^{(1)},z^{(1)},r^{(2)},z^{(2)},r^{(3)},z^{(3)}]^T$ and Φ_{iB} is the shape function matrix given by

$$\mathbf{\Phi} = \begin{bmatrix} \phi^1(R,Z) & 0 & \phi^2(R,Z) & 0 & \phi^3(R,Z) & 0 \\ 0 & \phi^1(R,Z) & 0 & \phi^2(R,Z) & 0 & \phi^3(R,Z) \end{bmatrix}. \tag{78}$$

Here $\phi^j(R,Z)$ is a shape function with respect to the jth nodal point and the shape functions satisfy $\sum_j^{(all\ nodes)}\phi^j(R,Z)=1$.

Variations are given in terms of the directional derivative (Gâteaux derivative)

$$\delta_{(\mathbf{x})}f(\mathbf{x}) = \left.\frac{d(f(\mathbf{x}+\varepsilon\delta\mathbf{x}))}{d\varepsilon}\right|_{\varepsilon=0}. \tag{79}$$

In a Galerkin treatment, the shape function itself is typically chosen as a weight function (i.e., $\delta x_i = \Phi_{iA}$). Using the chain-rule, the variational operation can be expressed with respect to the nodal position vectors as

$$\delta_{(\mathbf{x})}f(\mathbf{x}) = \left.\frac{d(f(x_B^p\Phi_{iB}+\varepsilon_A\Phi_{iA}))}{d\varepsilon_A}\right|_{\varepsilon_A=0} = \frac{\partial f(\mathbf{x})}{\partial x_A^p}. \tag{80}$$

Thus, the finite element formulation (76) can be written in the form

$$[\mathcal{F}_{(\mathbf{x})}]_A = \iint\left\{\frac{\partial \hat{\Psi}}{\partial C_{\alpha\beta}}\frac{\partial C_{\alpha\beta}}{\partial x_A^p} + \hat{H}'(J)\frac{\partial J}{\partial C_{\alpha\beta}}\frac{\partial C_{\alpha\beta}}{\partial x_A^p}\right\}(R\, dR\, dZ) + \int t_k^o\hat{\Phi}_{kA}(R\, dS) = 0, \tag{81}$$

where $dS^2=dR^2+dZ^2$. Eq. (81) are solved by using Newton–Raphson iteration

$$\{\mathbf{x}^p\}^{n+1} = \{\mathbf{x}^p\}^n - \left[\frac{\partial \mathcal{F}_{(\mathbf{x})}}{\partial \mathbf{x}^p}\right]^{-1}\{\mathcal{F}_{(\mathbf{x})}\}, \tag{82}$$

where

$$\frac{\partial[\mathcal{F}_{(\mathbf{x})}]_A}{\partial x_B^p} = \iint\left\{\frac{\partial^2\hat{\Psi}}{\partial C_{\alpha\beta}\partial C_{\gamma\omega}}\frac{\partial C_{\alpha\beta}}{\partial x_A^p}\frac{\partial C_{\gamma\omega}}{\partial x_B^p} + \frac{\partial \hat{\Psi}}{\partial C_{\alpha\beta}}\frac{\partial^2 C_{\alpha\beta}}{\partial x_A^p\partial x_B^p} + \hat{H}'(J)\frac{\partial^2 J}{\partial C_{\alpha\beta}\partial C_{\gamma\omega}}\frac{\partial C_{\alpha\beta}}{\partial x_A^p}\frac{\partial C_{\gamma\omega}}{\partial x_B^p} + \hat{H}'(J)\frac{\partial J}{\partial C_{\alpha\beta}}\frac{\partial^2 C_{\alpha\beta}}{\partial x_A^p\partial x_B^p}\right.$$

$$+\hat{H}''(J)\frac{\partial J}{\partial C_{\alpha\beta}}\frac{\partial J}{\partial C_{\gamma\omega}}\frac{\partial C_{\alpha\beta}}{\partial x_A^p}\frac{\partial C_{\gamma\omega}}{\partial x_B^p}\Big\}(R\,dR\,dZ) \tag{83}$$

and the derivatives of the Jacobian with respect to the Cauchy–Green stretch tensor are given by

$$\frac{\partial J}{\partial C_{\alpha\beta}}=\frac{J}{2}C^{-1}_{\alpha\beta}, \tag{84}$$

$$\frac{\partial^2 J}{\partial C_{\alpha\beta}C_{\gamma\omega}}=-\frac{J}{4}[C^{-1}_{\alpha\gamma}C^{-1}_{\beta\omega}+C^{-1}_{\alpha\omega}C^{-1}_{\beta\gamma}]+\frac{J}{4}C^{-1}_{\alpha\beta}C^{-1}_{\gamma\omega}. \tag{85}$$

For an unsaturated gel, the weak form is augmented so as to include the global constraint (60). Since $\int_{\Omega_{\varepsilon_{\mathbf{X}}}} JJ^s\,dV=\int_{\Omega_R} J\,dV$ the variational equation can be written

$$\int_{\Omega_R}\frac{\partial\hat{\Psi}}{\partial\mathbf{C}}:\delta\mathbf{C}+\hat{H}'(J)\frac{\partial J}{\partial\mathbf{C}}:\delta\mathbf{C}\,dV-\int_{\Gamma_t}\mathbf{t}\cdot\delta\mathbf{x}\,da-P\delta\left(\int_{\Omega_R}J\,dV-V_*\right)=0, \tag{86}$$

where V_* is the known total volume and the as yet unknown constant P is the associated Lagrange multiplier. Hence, one solves the following weak form equation

$$\int_{\Omega_R}\frac{\partial\hat{\Psi}}{\partial\mathbf{C}}:\delta\mathbf{C}+(\hat{H}'(J)-P)\frac{\partial J}{\partial\mathbf{C}}:\delta\mathbf{C}\,dV-\int_{\Gamma_t}\mathbf{t}\cdot\delta\mathbf{x}\,da=0, \tag{87}$$

with

$$\int_{\Omega_R}J\,dV-V_*=0. \tag{88}$$

To treat (87) and (88), one begins with an initial guess $P=P^0$ and solves (87) as in the case of a saturated gel. Then P is updated so as to converge upon (88) by Newton iteration, i.e.,

$$P^{n+1}=P^n-\frac{V(P^n)-V_*}{dV/dP}, \tag{89}$$

where $V(P^n)=\int_{\Omega_R}J\,dV$ is calculated from the solution of (87) with $P=P^n$ and dV/dP is its derivative with respect to P which is obtained numerically.

5.2. FE formulation for a 3D model

In a manner similar to that resulting in (81), governing equations for the 3D finite element formulation for the saturated gel are obtained as

$$[\mathcal{F}_{(\mathbf{x})}]_A=\int_{\Omega_R}\left\{\frac{\partial\hat{\Psi}}{\partial C_{\alpha\beta}}\frac{\partial C_{\alpha\beta}}{\partial x_A^p}+\hat{H}'(J)\frac{\partial J}{\partial C_{\alpha\beta}}\frac{\partial C_{\alpha\beta}}{\partial x_A^p}\right\}dV+\int_{\Gamma_t^o}t_k^o\hat{\Phi}_{kA}\,dA=0. \tag{90}$$

The tangent matrix for the Newton–Raphson method is then given by

$$\begin{aligned}\frac{\partial[\mathcal{F}_{(\mathbf{x})}]_A}{\partial x_B^p}=\int_{\Omega_R}\Bigg\{&\frac{\partial^2\hat{\Psi}}{\partial C_{\alpha\beta}\partial C_{\gamma\omega}}\frac{\partial C_{\alpha\beta}}{\partial x_A^p}\frac{\partial C_{\gamma\omega}}{\partial x_B^p}+\frac{\partial\hat{\Psi}}{\partial C_{\alpha\beta}}\frac{\partial^2 C_{\alpha\beta}}{\partial x_A^p\partial x_B^p}+\hat{H}'(J)\frac{\partial^2 J}{\partial C_{\alpha\beta}\partial C_{\gamma\omega}}\frac{\partial C_{\alpha\beta}}{\partial x_A^p}\frac{\partial C_{\gamma\omega}}{\partial x_B^p}\\&+\hat{H}'(J)\frac{\partial J}{\partial C_{\alpha\beta}}\frac{\partial^2 C_{\alpha\beta}}{\partial x_A^p\partial x_B^p}+\hat{H}''(J)\frac{\partial J}{\partial C_{\alpha\beta}}\frac{\partial J}{\partial C_{\gamma\omega}}\frac{\partial C_{\alpha\beta}}{\partial x_A^p}\frac{\partial C_{\gamma\omega}}{\partial x_B^p}\Bigg\}dV.\end{aligned} \tag{91}$$

Let $\{\mathbf{E}_1,\mathbf{E}_2,\mathbf{E}_3\}$ and $\{\mathbf{E}_1^e,\mathbf{E}_2^e,\mathbf{E}_3^e\}$ be orthonormal basis vectors in the global and local coordinates, respectively. Since the pre-stretch tensor $\mathbf{F}^s$ is given a matrix representation with respect to a polar coordinates in (72), we take basis vectors of the polar coordinate system to be the local basis. The center of an element $\mathbf{X}^c$ is then set to the origin $\mathbf{O}=\{0,0,0\}$ of the local coordinates. Then the normalized vector in the radial direction becomes $\mathbf{E}_1^e$, and $\{0,0,1\}$ is set to $\mathbf{E}_3^e$. $\mathbf{E}_2^e$ is obtained by the cross product of $\mathbf{E}_3^e$ and $\mathbf{E}_1^e$. A point $\mathbf{X}=\{X_1,X_2,X_3\}$ in the global Cartesian coordinate system is transformed to the local Cartesian coordinate $\mathbf{X}^e=\{X_1^e,X_2^e,X_3^e\}$ by

$$X_\alpha^e=\mathbf{E}_\alpha^e\cdot(\mathbf{X}-\mathbf{X}^c),\quad\text{or}\quad X_\alpha^e=Q_{\alpha\beta}(X_\beta-X_\beta^c), \tag{92}$$

where $Q_{\alpha\beta}=\mathbf{E}_\alpha^e\cdot\mathbf{E}_\beta$. A linear element has four nodal points and it is convenient to define vectors for the nodal points as

$$\mathbf{X}^{ep}=\{X_1^{e(1)},X_2^{e(1)},X_3^{e(1)},X_1^{e(2)},X_2^{e(2)},X_3^{e(2)},X_1^{e(3)},X_2^{e(3)},X_3^{e(3)},X_1^{e(4)},X_2^{e(4)},X_3^{e(4)}\}^T, \tag{93}$$

$$\mathbf{X}^{p}=\{X_1^{(1)},X_2^{(1)},X_3^{(1)},X_1^{(2)},X_2^{(2)},X_3^{(2)},X_1^{(3)},X_2^{(3)},X_3^{(3)},X_1^{(4)},X_2^{(4)},X_3^{(4)}\}^T. \tag{94}$$

Vectors $\mathbf{x}^{ep}$ and $\mathbf{x}^{p}$ can de defined in a similar fashion. The coordinate transform between the global and the local coordinates is given by

$$\mathbf{X}^{ep}=\tilde{\mathbf{Q}}(\mathbf{X}^{p}-\mathbf{X}^{cp}),\quad \mathbf{x}^{ep}=\tilde{\mathbf{Q}}(\mathbf{x}^{p}-\mathbf{X}^{cp}), \tag{95}$$

where $\tilde{Q}$ is a 12×12 matrix representing the rotation. The position vector in the local coordinate is

$$\mathbf{x}^{e}(X_1,X_2,X_3)=\mathbf{\Phi}\mathbf{x}^{ep} \tag{96}$$

where

$$\mathbf{\Phi}=\begin{bmatrix} \phi^1 & 0 & 0 & \phi^2 & 0 & 0 & \phi^3 & 0 & 0 & \phi^4 & 0 & 0\\ 0 & \phi^1 & 0 & 0 & \phi^2 & 0 & 0 & \phi^3 & 0 & 0 & \phi^4 & 0\\ 0 & 0 & \phi^1 & 0 & 0 & \phi^2 & 0 & 0 & \phi^3 & 0 & 0 & \phi^4 \end{bmatrix}, \tag{97}$$

and $\phi^j(X_1,X_2,X_3)$ is the shape function with respect to the jth nodal point. The shape functions satisfy $\sum_j^{(all\ nodes)}\phi^j(X_1,X_2,X_3)=1$. Using (95) and (96), the vector $\mathbf{x}^e$ can be written as

$$\mathbf{x}^{e}=\mathbf{\Phi}\tilde{\mathbf{Q}}(\mathbf{x}^{p}-\mathbf{X}^{cp}),\quad [x^{e}_{\alpha}=\Phi_{\alpha A}\tilde{Q}_{AB}(x^{p}_{B}-X^{cp}_{B})]. \tag{98}$$

Define $\mathbf{\Phi}^e$ by components as follows:

$$\Phi^{e}_{\alpha B}=\Phi_{\alpha A}\tilde{Q}_{AB}. \tag{99}$$

The deformation gradient and the right Cauchy–Green tensor then have component representations with respect to the local coordinates by

$$F_{\alpha\beta}=x^{e}_{\alpha,\beta}=\Phi^{e}_{\alpha A,\beta}x^{p}_{A},\quad C_{\alpha\beta}=x^{e}_{\gamma,\alpha}x^{e}_{\gamma,\beta}=\Phi^{e}_{\gamma A,\alpha}x^{p}_{A}\Phi^{e}_{\gamma B,\beta}x^{p}_{B}. \tag{100}$$

The spatial derivatives of $\mathbf{C}$ appearing in (91) now follow directly from differentiation of (100) with respect to the components of $\mathbf{x}^p$.

6. Eversion simulation by means of the FEM

For numerical simulation, consider a hollow cylinder such that $R^s_o=2R^s_i$ and $L^s=R^s_o$. These ratios are preserved by the free swelling (65). In addition, the deformation (68) which establishes locations in the computational domain then gives $R_o=2R_i$. The *lateral surfaces* are the particle points that are at $R=R_i$ and $R=R_o$ in Ω_R. The *upper cap* are the particles at $Z=\zeta L^s$ and the *lower cap* are the particles at $Z=0$ in Ω_R. As discussed in Wineman and Rajagopal (1992) and Deng and Pence (2010a) the parameter values $M=100\mu$ and $\chi=0.425$ are suggested by the work of Paul and Ebra-Lima on rubbers infused with toluene (Paul and Ebra-Lima, 1970), and these values will be used here as well so as to provide results that can be directly compared to those presented in Deng and Pence (2010a). For these parameter values it is found that the free swelling stretch takes on the value $\zeta=1.722$. Axisymmetric FEM uses the cross-section of the cylinder as shown in the right panel of Fig. 2 in which distances have been nondimensionalized by R_i. The left panel shows the 3D computational domain. A geometric mesh for both the 3D and the axisymmetric FEM was then created on these domains using HyperMesh (HyperWorks, Altair). The numerical computation as described in the previous section is then performed on Matlab. Various boundary conditions are now prescribed on the caps and lateral surfaces for both the case of a saturated gel and that of an unsaturated gel.

6.1. Simple eversions with no Z variation and verification with Deng and Pence (2010a)

As discussed in Section 4, the special eversion deformation in which there is no Z variation in the radial displacement is treated at length in Deng and Pence (2010a) by the previously indicated ODE method. Such a deformation is achievable with traction free lateral surfaces provided that the caps are maintained to be flat by a suitable distribution of normal tractions.

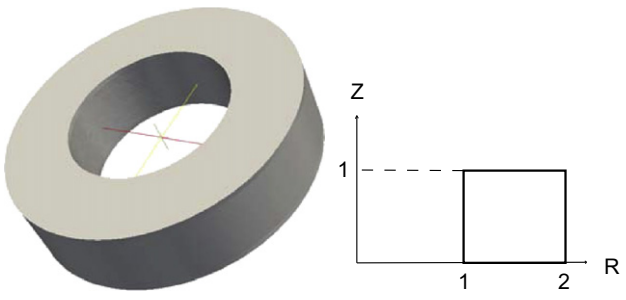

Fig. 2. A geometric model for finite element analysis. The inner and outer radii are 1 and 2, respectively, and the lateral length is 1. Left: a geometric model for 3D FEM, Right: the axisymmetric cross-section of the cylinder for 2D FEM.

Hence the boundary conditions for the corresponding FEM is that of traction free lateral surfaces and caps that are each subject to a uniform normal displacement and zero shear tractions. The polar coordinate system then provides a principal frame for the resulting deformation which, as shown in Deng and Pence (2010a) and discussed here in Section 4, can be described by $r=\tilde{r}(R^s)$ and $z=-\lambda_z Z^s=-\hat{\lambda}_z\zeta Z^s$ where we have introduced $\hat{\lambda}_z=\lambda_z/\zeta$. By this means the axial deformation is simply $z=\hat{\lambda}_z Z$ since $Z=-\zeta Z^s$ (viz. (65) and (68)). This permits the prescribed normal displacements to be expressed as zero on the lower cap and as $(\hat{\lambda}_z-1)L^s$ on the upper cap. Unlike Deng and Pence (2010a) it is to be emphasized that the FEM does not incorporate the deformation assumptions $r=\tilde{r}(R^s)$, $z=-\hat{\lambda}_z\zeta Z^s$ since it proceeds directly using the formulation described in Section 5.

The radial variation of $J_{g\mathbf{X}}$ (normalized by ζ^3), and the stress components (normalized by μ) from the axisymmetric FEM simulations are shown in Fig. 3 for the saturated material. Values are displayed for both $\hat{\lambda}_z=1$ and 2; they show very good agreement with the saturated condition results from Deng and Pence (2010a). As shown in the figure, the r domain is different for the two values of $\hat{\lambda}_z$ because r is the deformed radial location. The case $\hat{\lambda}_z=1$ keeps the caps at the same Z values as in the computational domain, however the lateral surfaces have each moved outward, which is again reflective of the fact that the computational domain is not itself in equilibrium without an appropriate distribution of external body forces. In contrast, the case $\hat{\lambda}_z=1$ displayed in Fig. 3 involves an equilibrated body (with nonzero stresses). The spatial variation in J is reflective of a nonuniform liquid content within the gel. The simulations show that relatively more fluid is located at the outer portion of the everted cylinder. As $\hat{\lambda}_z$ increases, the gel's local volume ($J_{g\mathbf{X}}/\zeta^3$) increases and hence the total amount of fluid absorbed within the body.

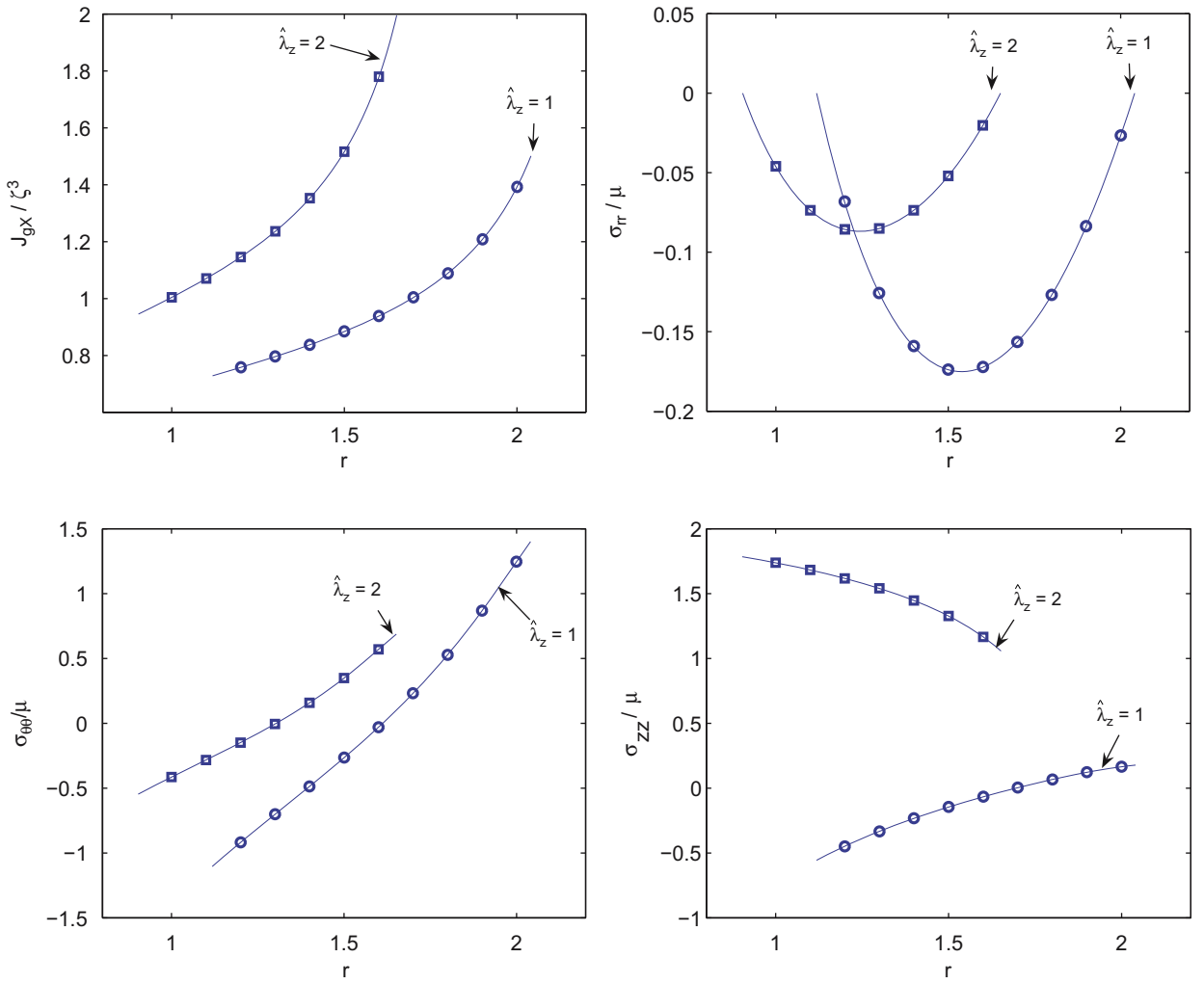

Fig. 3. Axisymmetric FEM simulation for a saturated gel compared to results from Deng and Pence (2010a) for imposed axial stretches $\hat{\lambda}_z$ on the swollen everted cylinder. Values of $J_{g\mathbf{X}}/\zeta^3$, σ_{rr}/μ, $\sigma_{\theta\theta}/\mu$, and σ_{zz}/μ are calculated along the line ($Z=\zeta L^s/2$) from the FEM results (3242 elements) and plotted with open squares and circles. The solid lines are results from the ODE analysis of Deng and Pence (2010a).

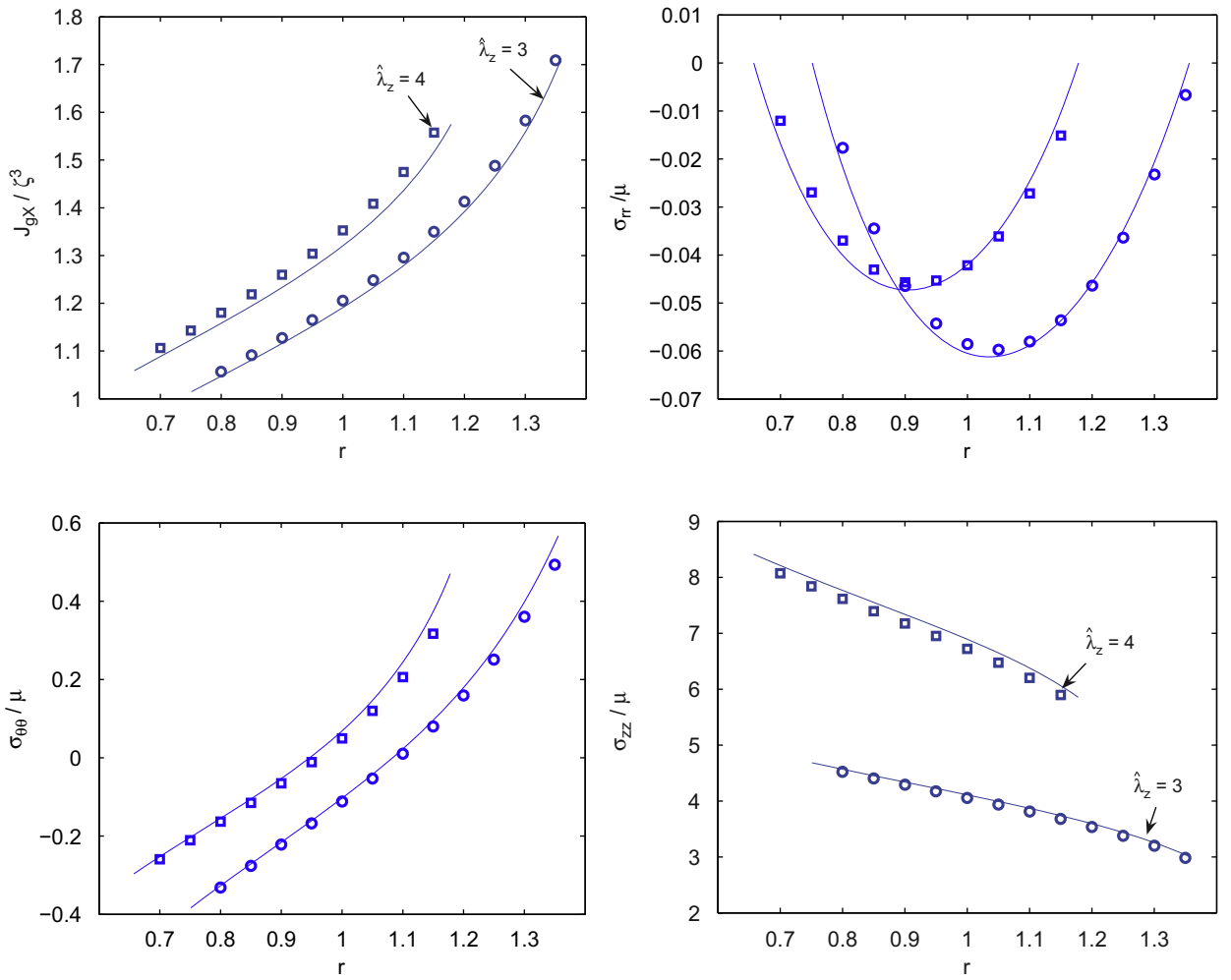

Fig. 4. Axisymmetric FEM simulation for an unsaturated gel subject to imposed axial stretch $\hat{\lambda}_z$ after eversion of the swollen cylinder. Open circles and squares are results from the FEM with $\hat{\lambda}_z = 3$ and 4 after loss-of-saturation, which is taken to occur at $\hat{\lambda}_z = 2$. The solid lines are the corresponding results from Deng and Pence (2010a).

If the overall amount of fluid in the system is limited, then all of the fluid could be absorbed within the body at some value of $\hat{\lambda}_z$. Following Deng and Pence (2010a) we assume that this occurs at $\hat{\lambda}_z = 2$. The total volume of the swollen body then remains constant as the cap displacement is subject to additional increase. In other words the body is now unsaturated for $\hat{\lambda}_z > 2$. Numerical results for the unsaturated material with $\hat{\lambda}_z = 3$ and 4 for loss-of-saturation at $\hat{\lambda}_z = 2$ are shown in Fig. 4. The results are again compared to corresponding results obtained in Deng and Pence (2010a) by the ODE procedure which assumes the special deformation form in which $r = \tilde{r}(R^s)$ and $z = -\hat{\lambda}_z \zeta Z^s$.

Results from the 3D FEM for the saturated gel with $\hat{\lambda}_z = 1$ are plotted in Fig. 5. Comparison with the results from Deng and Pence (2010a) show excellent agreement.

6.2. *More complex eversion deformations*

We now turn to consider more complex eversion deformations for which a nontrivial Z dependence no longer permits the ODE treatment of Deng and Pence (2010a). Fig. 6 depicts the saturated deformation corresponding to boundary conditions of fixed normal displacement and zero shear tractions on both the inner lateral surface and the lower cap. Specifically, the fixed normal displacements are taken as $r(R,Z)=R_i$ at $R=R_i$ and $z(R,Z)=0$ at $Z=0$. The remaining surfaces (the outer lateral boundary and the upper cap) are taken to be traction free. The traction free boundaries show significant deformation. Specifically, the inner lateral surface lengthens axially while the outer lateral surface is contracted. As in the case of the simpler deformations exhibited in Fig. 3 it remains the case that the outer periphery is higher in liquid content.

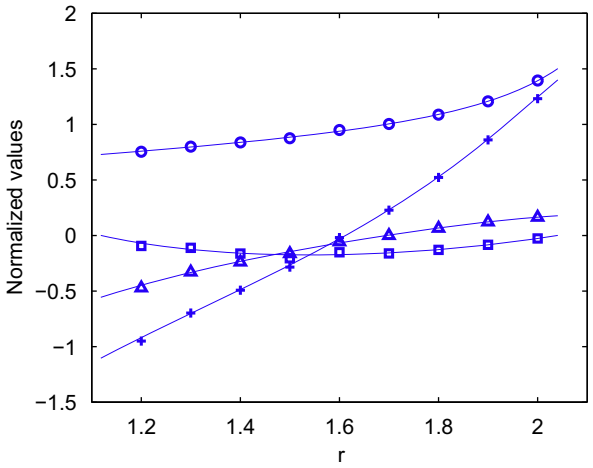

Fig. 5. 3D FEM (95150 elements) for normal displacement boundary conditions corresponding to $\hat{\lambda}_z = 1$, i.e., $z(X,Y,Z)$=0 at Z=0 and $z(X,Y,X)$=1 at Z=1. Normalized values $J_g\mathbf{x}/\zeta^3$ (open circle), σ_{rr}/μ (open square), $\sigma_{\theta\theta}/\mu$ (plus), and σ_{zz}/μ (open triangle) are calculated from the FEM results along the line: y=0 and z=0.5, and compared with the results from Deng and Pence (2010a) (solid lines).

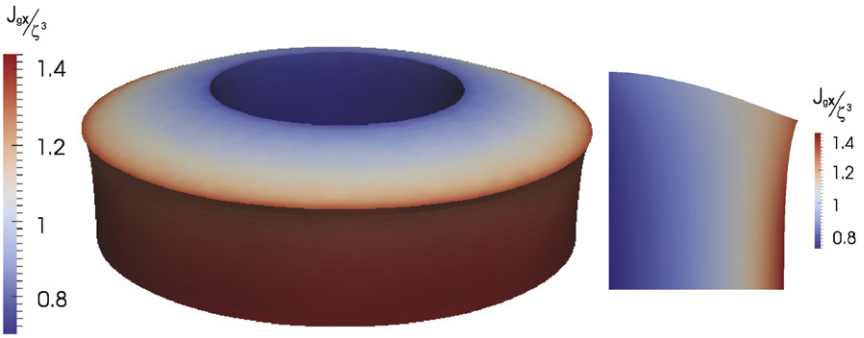

Fig. 6. A saturated deformation with boundary displacement constraints $r|_{R=R_i} = R_i$ and $z|_{Z=0} = 0$, from 3D FEM (left) and the axisymmetric FEM (right).

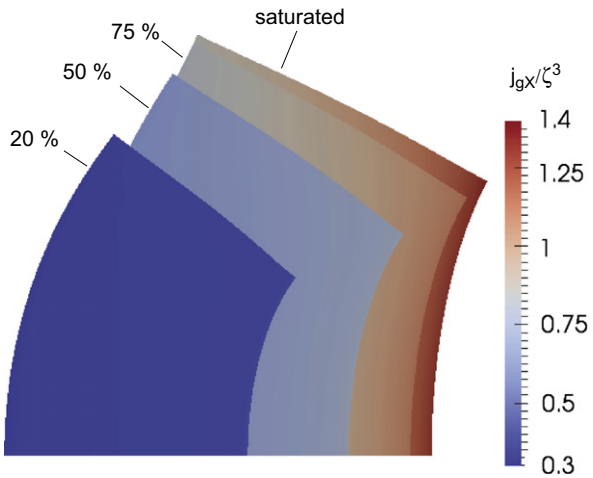

Fig. 7. An everted tube under saturated and unsaturated conditions. The boundary conditions are: traction free lateral surfaces, a traction free upper cap, and a lower cap that is free of shear traction while subject to the fixed normal displacement condition $z|_{Z=0} = 0$.

If, for the deformation depicted in Fig. 6, the boundary condition on the inner lateral surface is changed from one of prescribed normal displacement to one of zero normal traction, then that surface also becomes a free surface (like the outer lateral surface and the upper cap). This results in additional deformation as shown in Fig. 7. As regards the stresses, it is found

that the hoop stress $\sigma_{\theta\theta}$ is much larger in magnitude than the other two principal stresses σ_{rr} and σ_{zz}. The dependence of the hoop stress upon r along the bottom cap is shown in Fig. 8. This stress is compressive for small r and tensile for large r. This trend persists throughout the cylinder, although on the top cap one finds that the compressive zone is relatively smaller.

Fig. 7 also shows three different unsaturated deformations associated with these same boundary conditions. The corresponding hoop stress distributions are also shown in Fig. 8. Rather than indicating values for V_* in these figures, we present results in terms of the total volume of fluid V_f within the system (recall that the total volume of polymer is V_p as defined in (59)). There is sufficient liquid to saturate the freely swollen system provided that $V_f \geq (\zeta^3-1)V_p$. If there is insufficient liquid to provide for a freely swollen saturated system, then we may define the free swelling fluid volume fractional percentage $(\zeta^3-1)^{-1}V_f/V_p \times 100$ as a measure of undersaturation with respect to the freely swollen state. Specifically, Fig. 7 shows the unsaturated deformation when 75%, 50%, and 20% of the amount of fluid necessary for free swelling saturation is actually available and absorbed. It is to be remarked that the calculation for the unsaturated case becomes unstable as this percentage approaches zero; consequently the numerical implementation ceases to converge as $V_f \to 0$. This singularity issue in FEM simulation is also discussed in Hong et al. (2009). The offset in every fifth data point on the 20% curve in Fig. 8 seems to be connected to this effect.

Finally, we simulate the deformation sequence between an everted tube and the original free swollen state by a continuous process of equilibrium deformations. Fig. 9 shows different stages of such a process for a saturated tube using the 3D FEM. Each stage in the process is an equilibrium deformation such that both lateral surfaces are traction-free while the caps are subject to displacement boundary conditions which, in effect, turn the tube inside-out. The leftmost cross-sectional

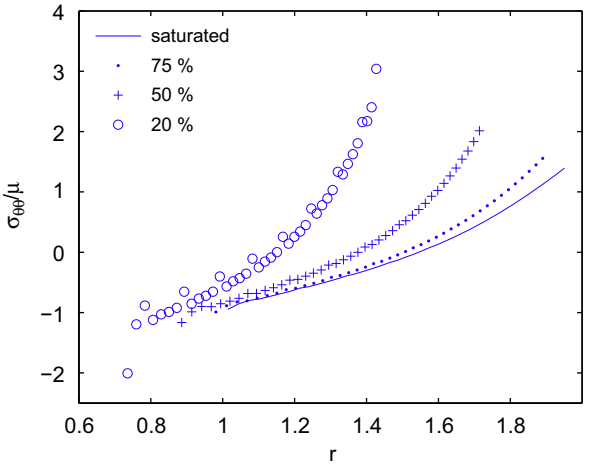

Fig. 8. Stress distribution $\sigma_{\theta\theta}$ as a function of r on the lower cap Z=0 for the deformations depicted in Fig. 7.

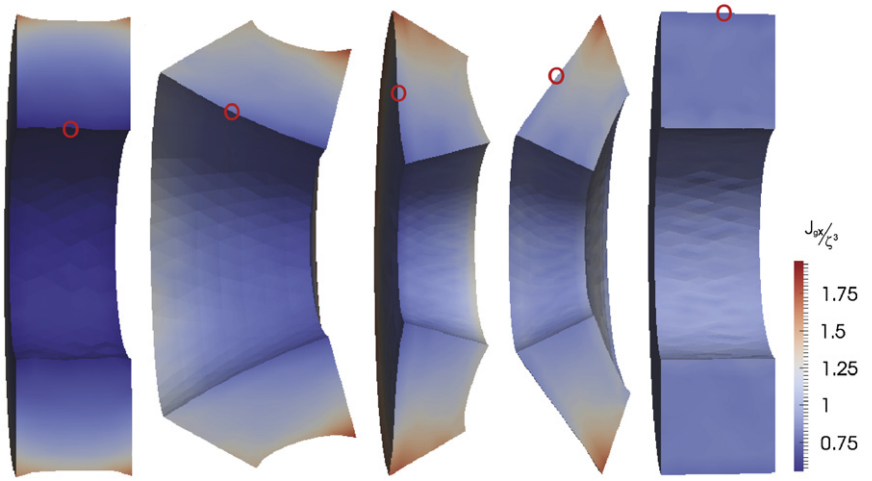

Fig. 9. The everted tube is computationally returned back to the original freely swollen state by rotating both of the caps using the 3D FEM. The red circle traces the inner boundary R=R_i of the computational domain, which returns to the outer boundary $R^{fs} = \zeta R_o^s$ of the freely swollen tube when the process is complete. (For interpretation of the references to color in this figure legend, the reader is referred to the web version of this article.)

view in Fig. 9 gives the everted tube and so the elements (if shown) would display minimal distortion. As the sequence proceeds from left to right these elements, if shown, would become progressively distorted. The normalized volume ($J_{g\mathbf{X}}/\zeta^3$) exhibits various changes as the process proceeds, which corresponds to redistribution of the fluid within the gel. The rightmost cross-section corresponds to the free swollen state formally described by (65) in which the value of $J_{g\mathbf{X}}$ is uniformly equal to ζ^3. Reading the figure from right to left corresponds to supplying boundary displacements that provide for an eversion of an originally freely swollen stress-free tube. The deformation sequence from the everted saturated tube to the saturated freely swollen state is also simulated using the axisymmetric FEM in the top panels of Fig. 10. The bottom panels show the corresponding deformation sequence for an unsaturated system in which 75% of the amount of fluid necessary for free swelling is available.

To gauge the mechanical effect of loss-of-saturation for this process, define an *everting moment* per unit angle θ as

$$M_\theta = \int_{\partial\Omega} |(\mathbf{x}-\mathbf{x}_c)\times\mathbf{t}| r\, dr\, dz \quad \text{where } \mathbf{x}_c = \frac{\int_\Omega \mathbf{x} r\, dr\, dz}{\int_\Omega r\, dr\, dz} \tag{101}$$

and $\mathbf{t}$ denotes the traction vector on the boundary. Here Ω is the 2D cross-section of the axisymmetric gel, $\partial\Omega$ is its boundary, and $\mathbf{x}_c$ is its centroid. Fig. 11 exhibits this moment during the deformation sequence for both the saturated case and for

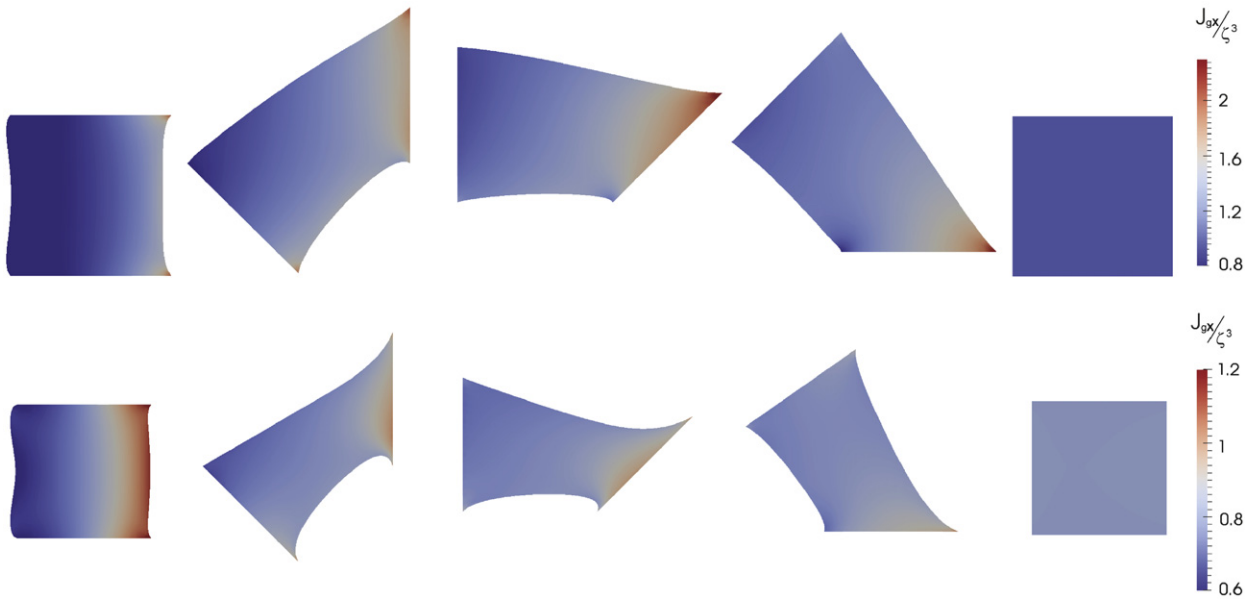

Fig. 10. The everted tube is computationally returned back to the original freely swollen state for the saturated (top) and unsaturated condition (bottom) by rotating both of the caps using the 2D axisymmetric FEM.

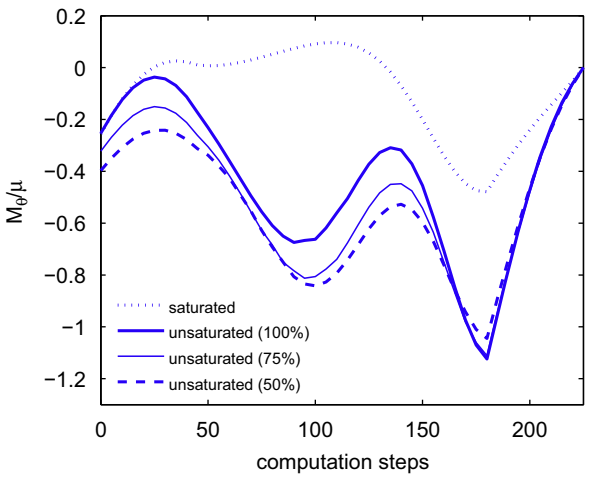

Fig. 11. The everting moment M_θ/μ per unit angle during the eversion.

different unsaturated cases corresponding to various amounts of available fluid. For the unsaturated case, liquid can neither enter nor leave during the deformation and this is found to increase the magnitude of the everting moment. Hence, as discussed in Deng and Pence (2010a,b), loss of saturation gives rise to an effective stiffness increase.

Fig. 11 also shows an unsaturated curve labeled 100% and this curve is quite different from the saturated curve. To explain the meaning of the 100%-curve consider first the total gel volume associated with the saturated deformation sequence. This total gel volume varies during the saturated deformation sequence since there is no volume constraint on the saturated gel. Using the result of the FEM to calculate this saturated volume, one finds that it is initially less than the free swelling volume but then at some point in the sequence it becomes greater than the free swelling volume. It then remains greater than the free swelling volume for the rest of the sequence, only returning to the free swelling volume at the conclusion of the sequence when the final state is that of a freely swollen uneverted tube. Now consider the system with overall liquid content that exactly corresponds to a freely swollen gel. The gel in this "100% system" will be saturated for the portion of the sequence when the saturated tube has a volume that is less than that of the freely swollen tube. This is because sufficient liquid is available in the 100% system to maintain such a volume. However, during the latter portion of the deformation sequence, when saturation requires more liquid than that of the freely swollen system, it will then be the case that the 100% system will be unsaturated. The 100%-curve in Fig. 11 is computed on such a basis. Hence the curve is initially coincident with the saturated curve. However, upon loss-of-saturation the curve departs from the saturation curve. After this departure its qualitative form is essentially the same as that of all of the other unsaturated curves.

7. Summary

In this work we examine swollen deformations for elastomeric gels subject to surface tractions. The gel is described as a mixture in which both the porous solid constituent and the interstitial liquid co-occupy each point of the material. Swelling is due to an increase in the amount of liquid constituent. These aspects are all quite standard in continuum mixture theory. Attention is focussed upon equilibrium states, so that there is no motion of the liquid constituent with respect to the solid constituent. Since we examine the effect of changing the boundary conditions upon the gel surface, such boundary conditions are viewed as varying sufficiently slowly so as to be consistent with a process such that each deformation in the sequence is equilibrated. In particular, we do not treat non-equilibrium dynamical processes, such as the migration of the interstitial liquid with respect to the deforming porous solid. Such dynamical processes are regarded as taking place and concluding on much faster time scales than that associated with changes to the applied tractions.

Instead our interest is on examining three situations corresponding to different ways in which the gel interacts with its external environment. The first is that of a saturated gel; this occurs when the gel is immersed in a bath of its liquid constituent. Changes in the applied traction will then generally alter the overall amount of liquid within the gel. The second is that in which the gel's external surface is in contact with a vapor phase of its liquid constituent. The third is that in which the liquid constituent does not pass through the gel's external surface so that the total amount of liquid constituent within the gel is fixed. This third situation is useful in modeling an unsaturated gel, meaning a gel that has less overall liquid content than that required for a saturated deformation. Governing equations and boundary conditions associated with these various situations are obtained through the use of a variational procedure described by Baek and Srinivasa (2004a).

A finite element method is created on the basis of the variational method and demonstrated for both saturated and unsaturated deformations. For an unsaturated deformation, the degree of undersaturation – a measure of the amount of liquid that would restore a state of saturation – affects the subsequent mechanical behavior. Specifically, the mechanical response stiffens as the overall amount of liquid within the gel is reduced. The cylindrical eversion deformation (turning a tube inside-out) is examined in some detail. In certain cases, as determined by the amount of available liquid, a loss-of-saturation can occur during the eversion processes. This greatly increases the torque which must be supplied per unit polar angle on the ends of the tube.

The variational procedure also clarifies the relation between an unsaturated gel and a gel that is in equilibrium with its vapor phase. The former may eventually transition to the latter if the unsaturated system is allowed to condense or evaporate its liquid component at the gel surface. The transition between the unsaturated case and the case of being in equilibrium with the vapor phase corresponds to the chemical potential variable of the gel changing its value from one that is determined by the original liquid content to the value of the chemical potential in the vapor phase.

References

Ambrosi, D., Preziosi, L., Vitale, G., 2010. The insight of mixtures theory for growth and remodeling. Z. Angew. Math. Phys. 61, 177–191.
Baek, S., Srinivasa, A.R., 2004a. Diffusion of a fluid through an elastic solid. Int. J. Non-Linear Mech. 39, 201–218.
Baek, S., Srinivasa, A.R., 2004b. Modeling of the pH-sensitive behavior of an ionic gel in the presence of diffusion. Int. J. Non-Linear Mech. 39, 1301–1318.
Ball, J.M., Schaeffer, D.G., 1993. Bifurcation and stability of homogeneous equilibrium configurations of an elastic body under dead-load tractions. Math. Proc. Cambridge Phil. Soc. 94, 315–339.
Bowen, R.M., 1980. Incompressible porous media models by use of the theory of mixtures. Int. J. Eng. Sci. 18, 1129–1148.
Bowen, R.M., 1982. Compressible porous media models by use of the theory of mixtures. Int. J. Eng. Sci. 20, 697–735.
Chen, Y.-C., Haughton, D.M., 1997. Existence of exact solutions for the eversion of elastic cylinders. J. Elasticity 49, 79–88.
Deng, H., Pence, T.J., 2010a. Equilibrium states of mechanically loaded saturated and unsaturated polymer gels. J. Elasticity 99, 39–73.
Deng, H., Pence, T.J., 2010b. Shear induced loss of saturation in a fluid infused swollen hyperelastic cylinder. Int. J. Eng. Sci. 48, 624–646.

Duda, F.P., Souza, A.C., Fried, E., 2010. A theory for species migration in a finitely strained solid with application to polymer network swelling. J. Mech. Phys. Solids 58, 515–529.
Flory, P., Rehner, J., 1943. Statistical mechanics of cross-linked polymer networks, 2. Swelling. J. Chem. Phys. 11, 521–543.
Gandhi, M.V., Rajagopal, K.R., Wineman, A.S., 1987. Some nonlinear diffusion problems within the context of the theory of interacting continua. Int. J. Eng. Sci. 25 (11–12), 1441–1457.
Gandhi, M.V., Usman, M., Wineman, A.S., Rajagopal, K.R., 1989. Combined extension and torsion of a swollen cylinder within the context of mixture theory. Acta Mech. 79, 81–95.
Gupta, P., Vermani, K., Garg, S., 2002. Hydrogels: from controlled release to pH-responsive drug delivery. Drug Discovery Today 7, 569–579.
Gurtin, M., 2000. Configurational Forces as Basic Concepts of Continuum Physics. Springer, New York.
Haughton, D.M., Orr, A., 1996. Further results for the eversion of highly compressible elastic cylinders. Math. Mech. Solids 1, 355–367.
Haughton, D.M., Orr, A., 1997. On the eversion of compressible elastic cylinders. Int. J. Solids Struct. 34, 1893–1914.
Hong, W., Zhao, X., Zhou, J., Suo, Z., 2008. A theory of coupled diffusion and large deformation in polymeric gels. J. Mech. Phys. Solids 56, 1779–1793.
Hong, W., Zhou, J., Suo, Z., 2009. Inhomogeneous swelling of a gel in equilibrium with a solvent and mechanical load. Int. J. Solids Struct. 46, 3282–3289.
Huggins, M.L., 1942. Theory of solutions of high polymers. J. Am. Chem. Soc. 64, 1712–1719.
Lee, K., Mooney, D., 2001. Hydrogels for tissue engineering. Chem. Rev 101, 1869–1880.
Nguyen, K., West, J., 2002. Photopolymerizable hydrogels for tissue engineering applications. Biomaterials 23, 4307–4314.
Paul, D.R., Ebra-Lima, O.M., 1970. Pressure-induced diffusion of organic liquids through highly swollen polymer membranes. J. Appl. Polym. Sci. 14, 2201–2224.
Qiu, Y., Park, K., 2001. Environment-sensitive hydrogels for drug delivery. Adv. Drug Deliver. Rev. 53, 321–339.
Rajagopal, K., Tao, L., 1996. Mechanics of Mixtures. World Scientific, Singapore.
Rivlin, R., 1977. Some research directions in finite elasticity. Rheol. Acta 16, 101–112.
Rivlin, R.S., 1949. Large elastic deformation of isotropic materials. vi. further results in the theory of torsion, shear and flexure. Phil. Trans. R. Soc. A 242 (845), 173–195.
Treloar, L., 1975. The Physics of Rubber Elasticity. Oxford University Press.
Treloar, L.R.G., 1950. The equilibrium swelling of cross-linked amorphous polymers. Phil. Trans. R. Soc. A 200, 176–183.
Wineman, A.S., Rajagopal, K.R., 1992. Shear induced redistribution of fluid within a uniformly swollen nonlinear elastic cylinder. Int. J. Eng. Sci. 30 (11), 1583–1595.